induce virus-specific CTLs that effectively eliminate virus-infected cells [18]. Since the liposomal conjugates induced CTLs efficiently when CTL epitope peptides were coupled to the surfaces of liposomes [17], the liposomal conjugatesare expected to be applicable for the development of CTL-based peptide vaccines. In the development of peptide vaccines, it is essential to know whether a T helper epitope peptide is necessary for the induction of long-lived memory $CD8^+$ T cells, an important step in vaccine preparation. This study was aimed at evaluating the role of $CD4^+$ T cells in the induction of long-lived memory $CD8^+$ T cells by liposome-coupled peptides.

Results

Induction of antigen-specific primary $CD8^+$ T cells and CTLs in mice by $OVA_{257-264}$-liposome conjugates

Mice were immunized with $OVA_{257-264}$-liposome conjugates in the presence of CpG as described in Materials and Methods. A significant induction of CTL specific for $OVA_{257-264}$ was observed on day 4 and a complete cell killing was observed as early as 5 days after the immunization (Figure 1). Therefore, in the following experiments, primary CTL responses were monitored at 7 days after immunization. Mice were then immunized with serially diluted solution of $OVA_{257-264}$-liposome conjugates containing 0.3 (8×) to 2.4 μg (1×) of peptides or $OVA_{257-264}$ solution that contained equal amounts of peptides as those in liposomal conjugates. Although $OVA_{257-264}$-liposome and $OVA_{257-264}$ solution seemed to induce a comparable level of T-cell cytokine production at the highest dose (2.4 μg/injection), a dose-dependent decrease was observed in mice immunized with $OVA_{257-264}$ solution but not in mice immunized with $OVA_{257-264}$-liposome, suggesting that $OVA_{257-264}$-liposome was more effective than $OVA_{257-264}$ solution in the induction of antigen-specific $CD8^+$ T cell cytokine production (Figure 2A). Similar results were observed in T cell cytokine production; a dose of $OVA_{257-264}$-liposome as low as 0.6 μg/mouse (4× dilution) induced a perfect killing as assayed by *in vivo* CTL assay, while $OVA_{257-264}$ solution induced only a partial killing even at the highest dose (Figure 2B).

Secondary CTL response in mice immunized with $OVA_{257-264}$-liposome

Induction of secondary CTL responses in mice immunized with $OVA_{257-264}$-liposome was further investigated. Mice were immunized with 50 μl of $OVA_{257-264}$-liposome and 2, 4, 8, 16, and 20

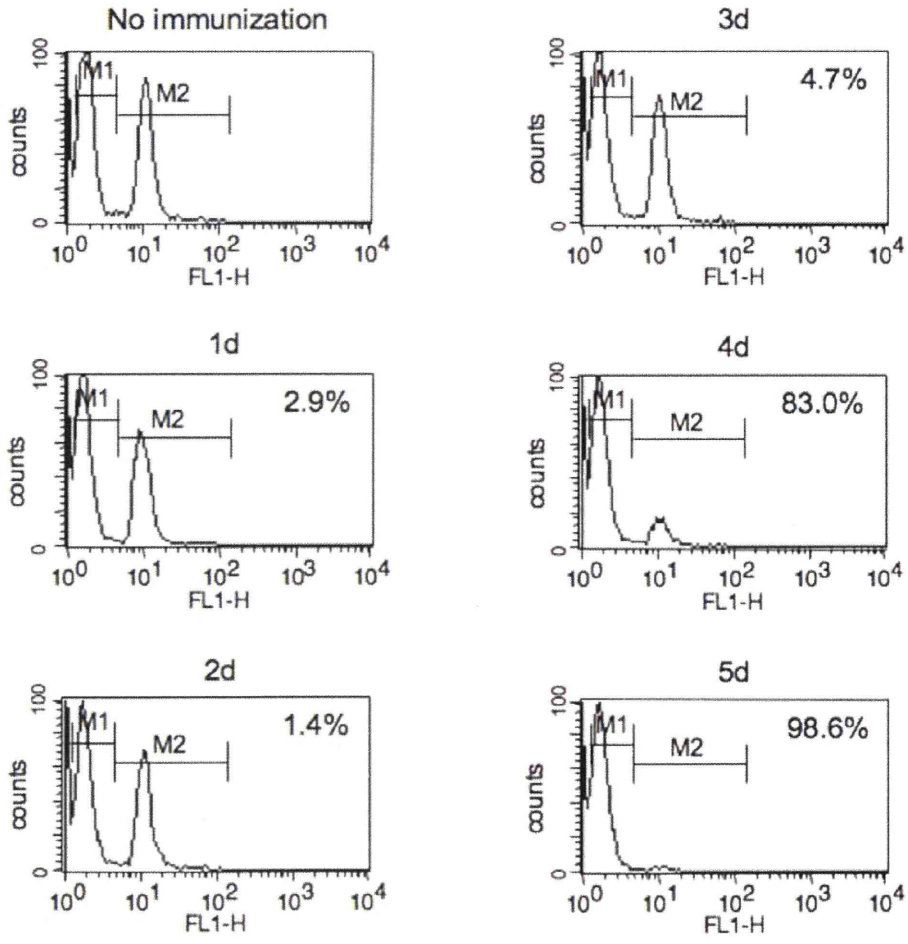

Figure 1. Kinetics of primary CTL response induced by $OVA_{257-264}$-liposome conjugates. Mice were immunized with 50 μl of $OVA_{257-264}$-liposome in the presence of 5 μg CpG; one to 5 days later, an *in vivo* CTL assay was performed as described in Materials and Methods. The numbers for each time period indicate percentages of target cells killed. Data are representative of three individual mice in each group for which similar results were obtained.
doi:10.1371/journal.pone.0015091.g001

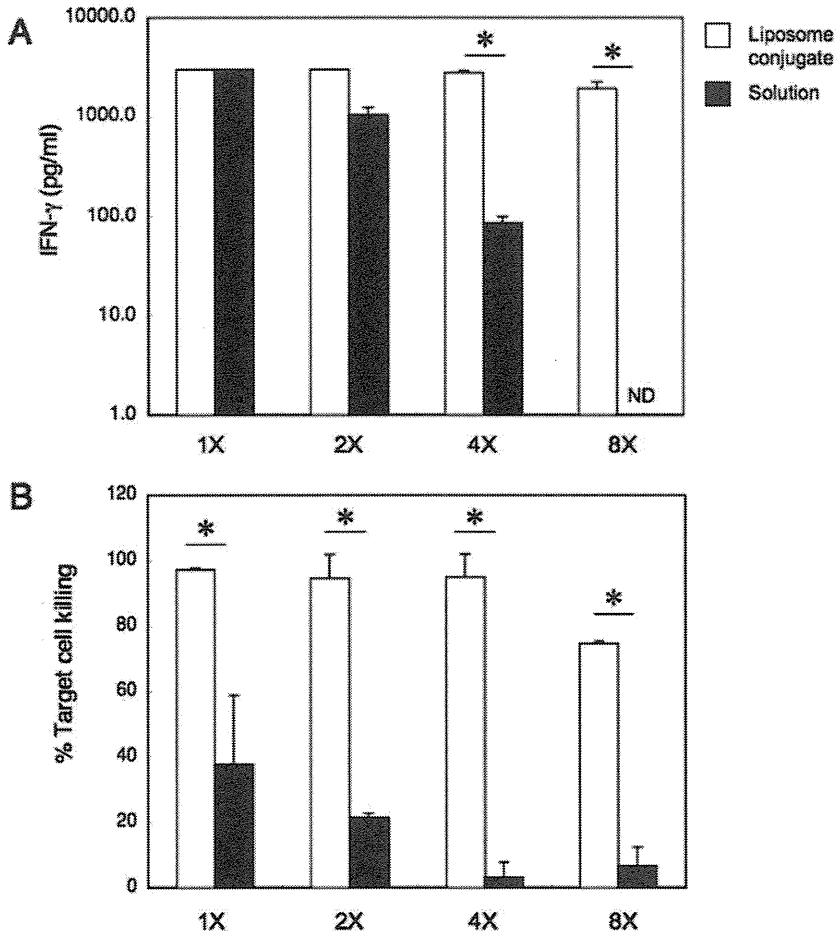

Figure 2. Dose-response of cytokine production by $CD8^+$ T cell and CTL induction in mice immunized with $OVA_{257-264}$-liposome or with $OVA_{257-264}$ solution. A serial two-fold dilution of $OVA_{257-264}$-liposome (open box) and $OVA_{257-264}$ solution (closed box) were made in PBS, and mice were immunized with the diluents in the presence of 5 μg CpG. $OVA_{257-264}$ solution containing equal amounts of peptides as those in $OVA_{257-264}$-liposome. One week after the immunization, IFN-γ production by $CD8^+$ T cells (**A**) and the CTL response (**B**) were monitored as described in Materials and Methods. Data represent means and SE of three mice per group. *, significant difference ($p>0.01$).
doi:10.1371/journal.pone.0015091.g002

weeks later, the mice received a booster injection with OVA. Three days after the booster injection, $OVA_{257-264}$-specific cell killing was monitored. As shown in Figure 3, a complete cell killing was observed at 2 weeks after the immunization without a booster injection and, up to 20 weeks after the immunization, a significant recall response was observed upon booster injection with OVA. Inoculation of naive mice with the same dose of OVA as the booster injection ("No imm." in Figure 3) did not induce a detectable CTL response. Interestingly, a significant recall response was observed even at 20 weeks when the primary CTL response was nearly undetectable. An antigen-specific $CD8^+$ T-cell proliferation assay further confirmed the results; as shown in Figure 4, $CD8^+$ T cells of mice immunized with $OVA_{257-264}$-liposome significantly proliferated upon *in vitro* stimulation with OVA even 20 weeks after immunization.

Effect of in vivo elimination with $CD4^+$ T cells on the induction of long-lived memory $CD8^+$ T cells by $OVA_{257-264}$-liposome conjugates

To eliminate $CD4^+$ T cells, mice were inoculated with GK1.5 as described in Materials and Methods, and immunized with $OVA_{257-264}$-liposome. As shown in Figure 5, *in vivo* elimination with $CD4^+$ T cells affected neither for primary (Figure 5A) nor for secondary (Figure 5B) CTL responses; even at 20 weeks after the immunization, a significant recall response, comparable to that in normal mice, was observed in mice from which $CD4^+$ T cells had been eliminated.

Discussion

In the present study, the role of $CD4^+$ T cells in the induction and maintenance of memory $CD8^+$ T cells was evaluated in mice immunized with liposome-coupled CTL epitope peptides. Although the inclusion of CpG, a ligand of TLR-9, was needed for the induction of the primary CTL response by $OVA_{257-264}$-liposome, $CD4^+$ T cells were not required in either primary or secondary response, since long-lived memory $CD8^+$ T cells were readily induced only by immunization with CTL epitope peptides coupled to liposomes (Figures 3 and 4). This finding was further confirmed in $CD4^+$ T cell-depleted mice (Figure 5). These results are in agreement with those reported previously by numerous investigators that $CD4^+$ T cells are dispensable for the primary expansion of $CD8^+$ T cells and their differentiation into cytotoxic

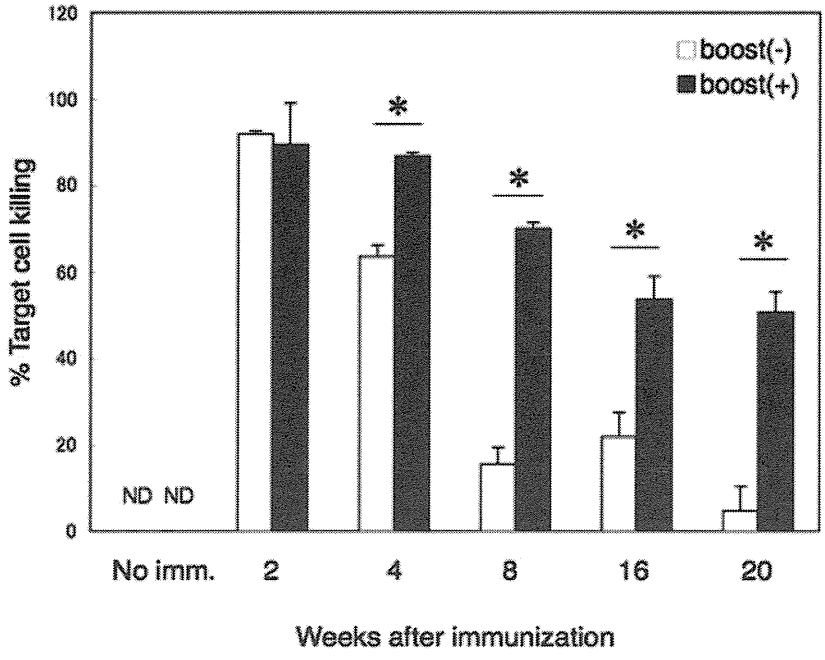

Figure 3. Secondary CTL response in mice immunized with $OVA_{257-264}$-liposome. Mice were immunized with 50 μl of $OVA_{257-264}$-liposome in the presence of 5 μg CpG, and 2, 4, 8, 16, and 20 weeks later, they received a booster ip injection with 200 μl of 1 mg/ml OVA in PBS (closed box) or no booster injection (open box). Three days after the booster injection, *in vivo* CTL assay was performed. Data represent mean percentages of cells killed and SEs of three mice per group. ND, not detected. *, significant difference ($p>0.01$).
doi:10.1371/journal.pone.0015091.g003

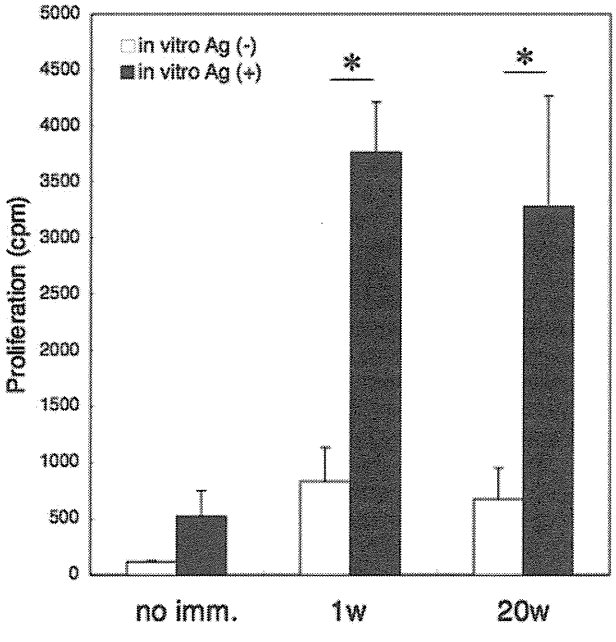

Figure 4. Antigen-specific $CD8^+$ T-cell proliferation assay. Mice were immunized with $OVA_{257-264}$-liposome and 1 week or 20 weeks later, $CD8^+$ T cells of the immunized mice were cultured in the presence (closed box) or absence (open box) of OVA as described in Materials and Methods. Data represents mean ^3H- thymidine incorporation and SE of triplicate cultures. *, significant difference ($p>0.01$).
doi:10.1371/journal.pone.0015091.g004

effectors [2,3,5]. However, most of these researchers have claimed that secondary CTL expansion is wholly dependent on the presence of T helper cells during, but not after, priming [1–5].

We previously reported that surface-linked liposomal antigens induced IgE-selective unresponsiveness [19]. The results were consistent even when different coupling procedures for the antigens with the liposomes were employed [20]. During the course of an investigation intended to clarify the mechanism of IgE-selective unresponsiveness induced by surface-coupled liposomal antigens, we discovered an alternative approach to regulating the production of IgE, one that is independent of the activity of T cells [21]. Immunization of mice with OVA-liposome conjugates induced IgE-selective unresponsiveness without apparent Th1 polarization. Neither interleukin-12 (IL-12), IL-10, nor $CD8^+$ T cells participated in the regulation. Further, $CD4^+$ T cells of mice immunized with OVA-liposome were capable of inducing antigen-specific IgE synthesis in athymic nude mice immunized with alum-adsorbed OVA. On the other hand, immunization of the recipient mice with OVA-liposome did not induce anti-OVA IgE production, even when $CD4^+$ T cells of mice immunized with alum-adsorbed OVA were transferred. In the secondary immune response, OVA-liposomes enhanced anti-OVA IgG antibody production but did not enhance ongoing IgE production, suggesting that the IgE-selective unresponsiveness induced by the liposomal antigen involved direct effects on IgE but not IgG switching *in vivo*. These results suggest the role of an alternative mechanism, one not involving T cells, in the regulation of IgE synthesis, and raise the possibility that the surface-linked liposomal antigens are potentially applicable for the development of novel vaccines with minimal induction of IgE synthesis. Moreover, given the relatively low allergic response to and increased antigenicity of the allergen, this form of antigen preparation would be applicable for allergen immunotherapy [22].

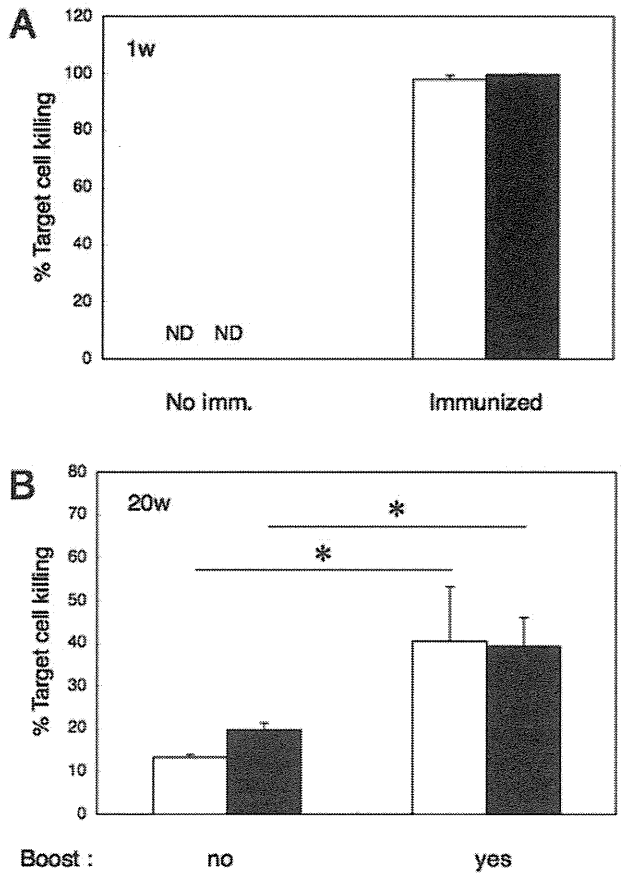

Figure 5. Effect of *in vivo* elimination of $CD4^+$ T cells on the induction of primary and secondary CTL responses by $OVA_{257-264}$-liposomes. Mice with (closed box) or without (open box) $CD4^+$ T-cell elimination were immunized with 50 μl of $OVA_{257-264}$-liposome solution in the presence of 5 μg CpG, and CTL induction was monitored. **A**, CTL response 1 week after immunization. **B**, CTL response 20 weeks after immunization with or without booster injection. *In vivo* CTL assay was performed 3 days after the booster injection. Data represent mean percent killing and SE of three mice per group. ND, not detected. *, significant difference ($p>0.01$).
doi:10.1371/journal.pone.0015091.g005

The potential usefulness of surface-linked liposomal antigens for application to vaccine development was further investigated. During the course of this investigation, a significant difference was observed in the recognition of liposomal antigens by antigen-presenting cells (APCs) between liposomes with different lipid components [23], and this difference was closely correlated with the adjuvant activity of liposomes [24]. In addition to this "quantitative" difference between liposomes with different lipid components, a "qualitative" difference (i.e., different abilities to induce cross-presentation) was also observed between liposomes with different lipid components [17]. Although the precise mechanism underlying this difference is currently unclear, the significant difference in membrane mobility observed between these liposomes [24] might affect their ability to induce cross-presentation. Thus, by utilizing their ability to induce cross-presentation, surface-linked liposomal antigens could be used to develop virus vaccines that induce a cytotoxic T-cell (CTL) response, as well as tumor vaccine preparations that present tumor antigens to APCs and induce effective antitumor responses [18].

Regarding the necessity of $CD4^+$ T cells in the generation of memory $CD8^+$ T cells, the results of the present study differed from those reported previously [1-5]. The difference in these findings may be due to differences in how mice were primed with antigens; in most of the studies reported previously, mice were primed by infecting viruses, such as LCMV [1,3,5], H3N2 influenza virus [2], and recombinant vaccinia virus [4], whereas in the present study, mice were immunized with OVA-derived CTL epitope peptides. Perhaps the difference in the requirements of $CD4^+$ T cells observed among those studies [1–5] and the present study was due to the difference in the efficiency of inducing the presentation of the immunodominant CTL epitope by APCs. In general, only ~1/2000 of the peptides in a foreign antigen expressed by an appropriate APC achieve immunodominant status with a given class I allele [25]. However, in the present study, immunization with $OVA_{257-264}$-liposome successfully induced both primary and secondary CTL responses without the presence of $CD4^+$ T cells (Figures 2 to 5). In addition, it was reported previously that antigens coupled to the surface of liposomes are recognized effectively by APCs and presented to T cells [24]. Therefore, although the TLR-ligand (CpG, in the present study) was necessary to mimic viral infection in order to induce CTL responses in the immunization with liposome-coupled peptides, $CD4^+$ T cells were not required for the induction and maintenance of $CD8^+$ memory T cells.

There is considerable interest in developing vaccines that elicit effective antiviral $CD8^+$ T cell responses [26] against a variety of viruses, such as HIV [27], HCV [28], and SARS coronavirus [29]. For this purpose, the utilization of the immunodominant CTL epitope would be more effective than the use of an attenuated, inactivated, or subunit vaccine in the development of virus vaccines to elicit effective antiviral $CD8^+$ T cell responses. For example, although the risk of a major global pandemic of avian influenza has created widespread concern, vaccines designed to induce antibodies against H5 haemagglutinin are expected to possess little or no efficacy, given the high rate of diversification of H5N1 strains due to the antigenic drift caused by point mutation of genes [30–33]. On the other hand, it is known that cytotoxic T cells specific for the internal proteins NP and M1 show high cross-reactivity between strains and between subtypes, reflecting high conservation of the internal proteins [34–37]. In addition, Lee et al. [38] recently reported that people who have not been exposed to H5N1 viruses have cross-reactive $CD8^+$ T cell memory to a wide range of H5N1 peptides. Therefore, these peptides are expected to be used to add a $CD8^+$ T cell component to current antibody-focused vaccine strategies with a view to reducing the impact of infection with novel influenza A viruses [39]. Epstein et al. [40] studied DNA vaccination in mice with plasmids expressing conserved nucleoprotein (NP) and matrix (M) from an H1N1 virus. However, the DNA vaccination alone protected poorly against a highly virulent strain of H5N1 influenza viruses.

Recently, we reported that peptides derived from the internal NP protein of the H3N2 influenza virus, chemically coupled to the surface of liposomes, induced antigen-specific CTLs and successfully inhibited the growth of H3N2 influenza virus in the lung [41]. More recently, we determined human HLA class I-restricted, immunodominant CTL epitopes derived from internal proteins of H5N1 influenza viruses [42]. Similar to those results reported previously [34–37,43], most of the CTL epitopes determined were well conserved and were identical with those involved in H1N1 and H3N2 influenza viruses. The combined use of these CTL epitope peptides, common to influenza viruses, and the surface-linked liposomal antigens which induce long-lived memory $CD8^+$ T cells without $CD4^+$ T cell help, was demonstrated to be

applicable for the development of a CTL-based influenza vaccine that is capable of inducing protection against heterosubtypic influenza viruses [42].

Taken together, these results suggest that surface-linked liposomal antigens might be applicable for the development of CTL-based vaccines to induce long-term prevention against infection with viruses other than influenza viruses, especially for those viruses that evade humoral immunity by varying their surface proteins, such as HIV, HCV, and SARS coronaviruses.

Materials and Methods

Mice

CBF1 mice (5–6 wk of age) were purchased from SLC (Shizuoka, Japan). All mice were maintained under specific pathogen-free conditions. Experiments in the present study were approved (permit numbers 208021 and 209082) by the Animal Research Committee of National Institute of Infectious Diseases, Tokyo, Japan and the mice were handled according to international guidelines for experiments with animals.

Chemicals

All phospholipids were obtained from NOF Co. (Tokyo, Japan). Reagent grades of cholesterol were purchased from Wako Pure Chemicals (Osaka, Japan).

Antigens and Reagents

Ovalbumin (OVA, grade VII) was purchased from Sigma-Aldrich. Mouse MHC class-I (K^b)-binding peptides $OVA_{257-264}$ (SIINFEKL) were obtained from Operon Biotechnologies (Tokyo, Japan). Synthetic CpG ODN (5002: TCCATGACGTTCTT-GATGTT), phosphorothioate-protected to avoid nuclease-dependent degradation, was purchased from Invitrogen.

Liposomes

The liposomes used in this study are provided by NOF corporation (Tokyo, Japan). They consisted of dioleoyl phosphatidylcholine (DOPC), dioleoyl phosphatidyl ethanolamine (DOPE), dioleoyl phosphatidyl glycerol (DOPG), and cholesterol in a 4:3:2:7 molar ratio. The crude liposome solution was passed through a membrane filter (Nucleopore polycarbonate filter; Coster) with a pore size of 0.2 μm.

Coupling of OVA peptides to liposomes

Liposomal conjugates with OVA peptides were prepared essentially in the same way as described previously [17] via disuccinimidyl suberate (DSS). Briefly, a mixture of 10 ml of anhydrous chloroform solution containing 0.136 mM DOPE and 24 μl of TEA was added in drops to 26.6 ml of anhydrous chloroform solution containing 0.681 mM DSS and stirred for 5 h at 40°C. The solvent was evaporated under reduced pressure, and 18 ml of a 2:1 mixture of ethyl acetate and tetrahydrofuran was added to dissolve the residue. Then, 36 ml of 100-mM sodium phosphate (pH 5.5) and 90 ml of saturated NaCl aqueous solution were added to the solution, shaken for 1 min, and allowed to separate. To remove undesirable materials, the upper layer was washed with the same buffer and, after evaporation of the solvent, 3 ml of acetone was added to dissolve the residue. One hundred ml of ice-cold acetone was added in drops and kept on ice for 30 min to precipitate. Crystals were collected and dissolved in 5 ml of chloroform. After evaporation, 34.4 mg of DOPE-DSS was obtained. Then, 0.18 mM DOPC, 0.03 mM DOPE-DSS, 0.21 mM cholesterol, and 0.06 mM DOPG were dissolved in 10 ml of chloroform/methanol. The solvent was removed under reduced pressure and 5.8 ml of phosphate buffer (pH 7.2) was added to make a 4.8% lipid suspension. The vesicle dispersion was extruded through a 0.2-μm polycarbonate filter to adjust the liposome size. A 2-ml suspension of DSS-introduced liposome and 0.5 ml of 5-mg/ml OVA peptide solution were mixed and stirred for 3 days at 4°C. The liposome-coupled- and uncoupled peptides were separated as described above using CL-4B column chromatography. The resulting solution of $OVA_{257-264}$-liposome conjugates contained 47 μg/ml of peptides as assessed by amino-acid quantitative analysis done by Toray Research Center (Kanagawa, Japan).

Immunization

All the mice were immunized with indicated doses of $OVA_{257-264}$-liposome conjugates via subctaneous injection in the presence of 5 μg/mouse CpG. For the booster immunization, the mice were immunized intraperitoneally (ip) with 200 μl of 1-mg/ml OVA in PBS solution.

In vivo elimination of $CD4^+$ T cells

For the *in vivo* elimination of $CD4^+$ T cells, mice received weekly ip injection with 0.5 mg of GK1.5, a monoclonal anti-CD4 antibody, throughout the experimental period. This treatment resulted in a >99% decrease in the number of $CD4^+$ T cells in the spleen and lymph nodes as determined by fluorescence-activated cell sorter (FACS) analysis.

In vivo cytotoxicity assay

Spleen cells of naive CBF1 mice were labeled with either 0.5 μM (dull) or 5 μM (bright) CFSE for 15 min at 37°C using a Cell Trace CFSE cell proliferation kit (Molecular Probes, Eugene, OR) and washed twice with ice-cold PBS. CFSE-bright cells were subsequently pulsed with 0.5 μg/ml of $OVA_{257-264}$ for 90 min at 37°C. CFSE-bright cells and CFSE-dull cells were mixed at a 1:1 ratio, and then a total of 1×10^6 cells was injected i.v. into the indicated group of mice. Twenty hours later, spleen cells were harvested from each mouse and analyzed by using FACSCalibur (Becton Dickinson, Mountain View, CA).

Cell culture

All incubations were performed in RPMI-1640 (Invitrogen Life Technologies) supplemented with 10% heat-inactivated FCS (HyClone), 100 U/ml penicillin, and 100 μg/ml streptomycin (Invitrogen).

Preparation of dendritic cells (DC) and $CD8^+$ T cells

DCs and $CD8^+$ T cells were obtained from spleen cells of CBF1 mice using the magnetic cell sorter system MACS according to the manufacturer's protocol using anti-CD11c and anti-CD8 antibody-coated microbeads (Miltenyi Biotec), respectively. $CD8^+$ T cells and DCs were suspended in RPMI-1640 containing 10% FCS at cell densities of 2×10^6/ml and 8×10^5/ml, respectively. The $CD8^+$ T cell suspension was plated at 250 μl per well onto 48-well culture plates (No. 3047; BD Biosciences), and 250 μl of DC suspension and 500 μl of 40 μM $OVA_{257-264}$ solution in the same medium were added to the plates. After incubation in a CO_2 incubator for 5 days, the culture supernatants were collected and assayed for the concentration of IFN-γ.

Cytokine assays

IFN-γ in the culture supernatant was measured using the Biotrak mouse ELISA system (GE Healthcare, UK). All test samples were assayed in duplicate, and the SE in each test was always less than 5% of the mean value.

T cell proliferation assay

Splenic $CD8^+$ T cells (5×10^5 cells/well) of immunized mice and whole spleen cells (1×10^5 cells/well) of 25 Gy-irradiated naïve mice were cultured in 96-well plates for 4 days in the presence (closed box) or absence (open box) of 20 μM OVA. The cells were pulsed with 1.25 μCi (0.046 MBq) [^{3}H]-thymidine (PerkinElmer) for the final 6 hours of the culture, and, after harvesting, cell proliferation was monitored using TopCount (PerkinElmer).

Statistical analysis

Student's *t* test was employed for the statistical analysis.

Author Contributions

Conceived and designed the experiments: TU. Performed the experiments: MT YT TK. Analyzed the data: MT TU. Contributed reagents/materials/analysis tools: MT YT. Wrote the paper: TU. N/A.

References

1. Matloubian M, Concepcion RJ, Ahmed R (1994) $CD4^+$ T cells are required to sustain $CD8^+$ cytotoxic T-cell responses during chronic viral infection. J Virol 68: 8056–8063.
2. Belz GT, Wodartz D, Diaz G, Nowak MA, Doherty PC (2002) Compromised influenza virus-specific $CD8^+$-T-cell memory in $CD4^+$-T-cell-deficient mice. J Virol 76: 12388–12393.
3. Janssen EM, Lemmens EE, Wolfe T, Christen U, von Herrath MG, et al. (2003) $CD4^+$ T cells are required for the secondary expansion and memory in $CD8^+$ T lymphocytes. Nature 421: 852–856.
4. Shedlock DJ, Shen H (2003) Requirement for CD4 T cell help in generating functional CD8 T cell memory. Science 300: 337–339.
5. Sun JC, Williams MA, Bevan MJ (2004) $CD4^+$ T cells are required for the maintenance, not programming, of memory $CD8^+$ T cells after acute infection. Nat Immunol 5: 927–933.
6. Bennett SR, Carbone FR, Karamalis F, Flavell RA, Miller JF, et al. (1998) Help for cytotoxic-T-cell responses is mediated by CD40 signaling. Nature 393: 478–480.
7. Bourgeois C, Rocha B, Tanchot C (2002) A role for CD40 expression on $CD8^+$ T cells in the generation of $CD8^+$ T cell memory. Science 297: 2060–2063.
8. Lee BO, Hartson L, Randall TD (2003) CD40-deficient, influenza-specific CD8 memory T cells develop and function normally in a CD40-sufficient environment. J Exp Med 198: 1759–1764.
9. Sun JC, Bevan MJ (2004) Long-lived CD8 memory and protective immunity in the absence of CD40 expression on CD8 T cells. J Immunol 172: 3385–3389.
10. Hernandez MG, Shen L, Rock KL (2007) CD40-CD40 ligand interaction between dendritic cells and $CD8^+$ T cells is needed to stimulated maximal T cell responses in the absence of $CD4^+$ T cell help. J Immunol 178: 2844–2852.
11. Heath WR, Carbone FR (2001) Cross-presentation, dendritic cells, tolerance and immunity. Annu Rev Immunol 19: 47–64.
12. Glenny AT, Pope CG (1926) Immunology notes. XXIII. The antigenic value of toxoid precipitated by potassium alum. J Pathol Bacteriol 29: 31–40.
13. Aggrebeck H, Wantzin J, Heon I (1996) Booster vaccination against diphtheria and tetanus in man: comparison of three different vaccine formations-III. Vaccine 14: 1265–1272.
14. Petrovsky N (2006) Novel human polysaccharide adjuvants with dual Th1 and Th2 potentiating activity. Vaccine 24 S2: 26–29.
15. Khajueia A, Gupta A, Singh S, Malik F, Singh J, et al. (2007) A new plant based vaccine adjuvant. Vaccine 25: 2706–2715.
16. Sun Y, Liu J (2008) Adjuvant effect of water-soluble polysaccharide (PAP) from the mycelium of Polyporus albicans on the immune responses to ovalbumin in mice. Vaccine 26: 3932–3936.
17. Taneichi M, Ishida H, Kajino K, Ogasawara K, Tanaka Y, et al. (2006) Antigens chemically coupled to the surface of liposomes are cross-presented to $CD8^+$ T cells and induce potent antitumor immunity. J Immunol 177: 2324–2330.
18. Uchida T, Taneichi M (2008) Clinical application of surface-linked liposomal antigens. Mini-Rev Med Chem 8: 184–192.
19. Naito S, Horino A, Nakayama M, Nakano Y, Nagai T, et al. (1996) Ovalbumin-liposome conjugate induces IgG but not IgE antibody production. Int Arch Allergy Immunol 109: 223–228.
20. Nakano Y, Mori M, Nishinohara S, Takita Y, Naito S, et al. (1999) Antigen-specific, IgE-selective unresponsiveness induced by antigen-liposome conjugates: comparison of four different conjugation methods. Int Arch Allergy Immunol 120: 199–208.
21. Taneichi M, Naito S, Kato H, Tanaka Y, Mori M, et al. (2002) T cell-independent regulation of IgE antibody production induced by surface-linked liposomal antigen. J Immunol 169: 4246–4252.
22. Uchida T (2003) Surface-linked liposomal antigen induces IgE selective unresponsiveness in a T-cell independent fashion. Cur Drug Targets Immune Endocr Metabol Disord 3: 119–135.
23. Nakano Y, Mori M, Yamamura H, Naito S, Kato H, et al. (2002) Cholesterol inclusion in liposomes affects induction of antigen-specific IgG and IgE antibody production in mice by a surface-coupled liposomal antigen. Bioconj Chem 13: 744–749.
24. Tanaka Y, Kasai M, Taneichi M, Naito S, Kato H, et al. (2004) Liposomes with differential lipid components exert differential adjuvanticity in antigen-liposome conjugates via differential recognition by macrophages. Bioconj Chem 15: 35–40.
25. Yewdell JW, Bennik JR (1999) Immunodominance in major histocompatibility complex class I-restricted T lymphocyte responses. Annu Rev Immunol 17: 51–88.
26. Yewdell JW, Haeryfar SM (2005) Understanding presentation of viral antigens to $CD8^+$ T cells in vivo: The key to rational vaccine design. Annu Rev Immunol 23: 651–682.
27. Watkins D (2008) The hope for an HIV vaccine based on induction of $CD8^+$ T lymphocytes. Mem Inst Oswaldo Cruz 103: 119–129.
28. Ishii S, Koziel MJ (2008) Immune responses during acute and chronic infection with hepatitis C virus. Clin Immunol 128: 133–147.
29. Zhu M (2004) SARS immunity and vaccination. Cell Mol Immunol 1: 193–198.
30. Guan Y, Poon LL, Cheung CY, Ellis TM, Lim W, et al. (2004) H5N1 influenza: A protean pandemic threat. Proc Natl Acad Sci 101: 8156–8161.
31. Webster RG, Govorkova EA (2006) H5N1 influenza - Continuing evolution and spread. N Engl J Med 355: 2174–2177.
32. Watanabe T, Watanabe S, Kim JH, Hatta M, Kawaoka Y (2008) Novel approach to the development of effective H5N1 influenza A virus vaccines: Use of M2 cytoplasmic tail mutants. J Virol 82: 2486–2492.
33. Skeik N, Jabr FI (2008) Influenza viruses and the evolution of avian influenza virus H5N1. Int J Infect Dis 12: 233–238.
34. Kreijtz JH, de Mutsert G, van Baalen CA, Fouchier RA, Osterhaus AD, et al. (2008) Cross-recognition of avian H5N1 influenza virus by human cytotoxic T-lymphocyte populations directed to human influenza A virus. J Virol 82: 5161–5166.
35. Heiny AT, Miotto O, Srinivasan KN, Khan AM, Zhang GL, et al. (2007) Evolutionarity conserved protein sequences of influenza a virus, avian and human, as vaccine targets. PLoS One 2: e1190.
36. Townsend ARM, Rothband J, Gotch FM, Bahadur G, Wraith D, et al. (1986) The epitopes of influenza nucleoprotein recognized by cytotoxic T lymphocytes can be defined with short synthetic peptides. Cell 44: 959–968.
37. Gotch F, McMichael A, Smith G, Moss B (1987) Identification of viral molecules recognized by influenza-specific human cytotoxic T lymphocytes. J Exp Med 165: 408–416.
38. Lee LY, Ann Ha DL, Simmons C, Jong MD, Chau NV, et al. (2008) Memory T cells established by seasonal human influenza A infection cross-react with avian influenza A (H5N1) in healthy individuals. J Clin Invest 118: 3478–3490.
39. Doherty PC, Kelso A (2008) Toward a broadly protective influenza vaccine. J Clin Invest 118: 3273–3275.
40. Epstein SL, Tumpey TM, Misplon JA, Lo CY, Cooper A, et al. (2002) DNA vaccin expressing conserved influenza virus proteins protective against H5N1 challenge infection in mice. Emerg Infect Dis 8: 796–801.
41. Nagata T, Toyota T, Ishigaki H, Ichihashi T, Kajino K, et al. (2007) Peptides coupled to the surface of a kind of liposome protect infection of influenza viruses. Vaccine 25: 4914–4921.
42. Matsui M, Kohyama S, Suda T, Yokoyama S, Mori M, et al. (2010) A CTL-based liposomal vaccine capable of inducing protection against heterosubtypic influenza viruses in HLA-A*0201 transgenic mice. Biochem Biophys Res Commun 391: 1494–1499.
43. Thomas PG, Keating R, Hulse-Post DJ, Doherty PC (2006) Cell-mediated protection in influenza infection. Emerg Infect Dis 12: 48–54.

OPEN ACCESS Freely available online

PLoS one

Liposome-Coupled Antigens Are Internalized by Antigen-Presenting Cells via Pinocytosis and Cross-Presented to CD8$^+$ T Cells

Yuriko Tanaka[1], Maiko Taneichi[2]*, Michiyuki Kasai[2], Terutaka Kakiuchi[1], Tetsuya Uchida[2]

1 Department of Immunology, Toho University School of Medicine, Tokyo, Japan, **2** Department of Safety Research on Blood and Biological Products, National Institute of Infectious Diseases, Tokyo, Japan

Abstract

We have previously demonstrated that antigens chemically coupled to the surface of liposomes consisting of unsaturated fatty acids were cross-presented by antigen-presenting cells (APCs) to CD8$^+$ T cells, and that this process resulted in the induction of antigen-specific cytotoxic T lymphocytes. In the present study, the mechanism by which the liposome-coupled antigens were cross-presented to CD8$^+$ T cells by APCs was investigated. Confocal laser scanning microscopic analysis demonstrated that antigens coupled to the surface of unsaturated-fatty-acid-based liposomes received processing at both MHC class I and class II compartments, while most of the antigens coupled to the surface of saturated-fatty-acid-based liposomes received processing at the class II compartment. In addition, flow cytometric analysis demonstrated that antigens coupled to the surface of unsaturated-fatty-acid-liposomes were taken up by APCs even in a 4°C environment; this was not true of saturated-fatty-acid-liposomes. When two kinds of inhibitors, dimethylamiloride (DMA) and cytochalasin B, which inhibit pinocytosis and phagocytosis by APCs, respectively, were added to the culture of APCs prior to the antigen pulse, DMA but not cytochalasin B significantly reduced uptake of liposome-coupled antigens. Further analysis of intracellular trafficking of liposomal antigens using confocal laser scanning microscopy revealed that a portion of liposome-coupled antigens taken up by APCs were delivered to the lysosome compartment. In agreement with the reduction of antigen uptake by APCs, antigen presentation by APCs was significantly inhibited by DMA, and resulted in the reduction of IFN-γ production by antigen-specific CD8$^+$ T cells. These results suggest that antigens coupled to the surface of liposomes consisting of unsaturated fatty acids might be pinocytosed by APCs, loaded onto the class I MHC processing pathway, and presented to CD8$^+$ T cells. Thus, these liposome-coupled antigens are expected to be applicable for the development of vaccines that induce cellular immunity.

Citation: Tanaka Y, Taneichi M, Kasai M, Kakiuchi T, Uchida T (2010) Liposome-Coupled Antigens Are Internalized by Antigen-Presenting Cells via Pinocytosis and Cross-Presented to CD8$^+$ T Cells. PLoS ONE 5(12): e15225. doi:10.1371/journal.pone.0015225

Editor: Derya Unutmaz, New York University, United States of America

Received August 3, 2010; **Accepted** November 1, 2010; **Published** December 17, 2010

Funding: This work was supported by grants from the Ministry of Health, Labor and Welfare of Japan (to TU), grants-in-aid for young scientists from the Japan Society for the Promotion of Science (21790963 to YT) and the research promotion grant from Toho University Graduate School of Medicine (No. 08-02 to YT). The funders had no role in study design, data collection and analysis, decision to publish, or preparation of the manuscript.

Competing Interests: The authors have declared that no competing interests exist.

* E-mail: taneichi@nih.go.jp

Introduction

Vaccines have played an important role in disease prevention and have made a substantial contribution to public health. Upon natural infection, it is known that the host responds by inducing both humoral and cellular immunity against the pathogen. However, most of the currently approved vaccines work by inducing humoral immunity [1–3]. For protection against viruses that are highly mutable and frequently escape from antibody-mediated immunity, such as influenza A viruses, HIV, and HCV, humoral immunity is insufficient [4–7]. Consequently, the development of vaccines that induce cellular immunity is critical to novel vaccine strategies.

T lymphocytes respond to peptide fragments of protein antigens that are displayed by MHC molecules on antigen-presenting cells (APCs). In general, extracellular antigens are presented via MHC class II molecules to CD4$^+$ T cells while intracellular antigens are presented via MHC class I molecules to CD8$^+$ T cells [8,9]. However, a number of reports have demonstrated that a significant level of crossover, so-called 'cross-presentation', occurs in APCs [10–14]. Using this phenomenon, novel vaccine preparation inducing antigen-specific CTLs that effectively eliminate virus-infected cells is expected. The mechanisms of cross-presentation have been studied intensively [15–17] while the details have been left unclear. Part of the antigens taken via phagocytosis by APCs are known to be translocated into the cytosol and degraded by local proteases [18,19]. In another pathway, some antigens internalized into endocytic compartments are loaded onto MHC class I molecules [20].

We previously reported that antigens chemically coupled to the surface of liposomes induced antigen-specific IgG but not IgE antibody production [21,22]. In addition, antigens chemically coupled to the surface of liposomes consisting of unsaturated fatty acids were presented not only to CD4$^+$- but also to CD8$^+$ T cells by APCs [23]. Since liposome-coupled antigens induce antiviral immunity [24,25], they are expected to be applicable for the development of viral vaccines without inducing antigen-specific IgEs, which cause allergic reactions. In the present study, we

investigated the mechanism by which the liposome-coupled antigens were cross-presented by APCs to $CD8^+$ T cells.

Results

Confocal laser scanning microscopic analysis of macrophages co-cultured with DQ-OVA-liposome conjugates

MHC class I of macrophages were stained with red fluorescein-labeled anti-mouse H-$2D^d$ mAb (Fig. 1A: left column), and MHC class II of macrophages were labeled with DM-DsRed (Fig. 1A: right column) as described in Materials and Methods. DQ-OVA, which exhibits green fluorescein upon proteolytic degradation, was coupled to liposomes consisting of unsaturated (oleoyl) or saturated (stearoyl) fatty acid, and added to the culture of macrophages. After incubation for 2 hr, the recovered macrophages were analyzed using confocal laser scanning microscopy. The results shown in Fig. 1 demonstrate that DQ-OVA coupled to oleoyl liposomes was processed at both MHC class I and class II compartments, while most of the DQ-OVA coupled to stearoyl liposomes was processed at the MHC class II compartment.

Differential manner of internalization by APCs of antigens coupled to liposomes with two kinds of lipid

$Alexa_{488}$-labeled OVA were coupled to liposomes and were added to the cultures of macrophages. As shown in Fig. 2, OVA coupled to oleoyl liposomes were internalized by APCs more efficiently than those coupled to stearoyl liposomes at 37°C. Interestingly, OVA coupled to oleoyl liposomes but not stearoyl liposomes were internalized significantly by APCs even in a 4°C environment.

Effect of inhibitors on uptake of liposome-coupled antigens by APCs

One of two kinds of inhibitors, cytochalasin B and DMA, which inhibit APC phagocytosis and pinocytosis of antigens, respectively, was added to the culture of macrophages 1 hr prior to the addition of $Alexa_{488}$-OVA- or DQ-OVA-coupled oleoyl liposomes. One hour later, flow cytometric analysis was performed. As shown in Fig. 3, the effect of cytochalasin B on the antigen uptake and digestion of liposome-coupled OVA by APCs was limited. On the other hand, DMA significantly reduced both antigen uptake and digestion of antigens by macrophages.

Localization of antigens coupled to liposomes in APCs

DQ-OVA-coupled oleoyl liposomes were added to the culture of macrophages in which either EEA1 or LAMP-1 were co-stained. The co-localization of the liposome-coupled antigens and intracellular organelles in the APCs was analyzed using confocal laser scanning microscopy. As shown in Figure 4, although most of the DQ-OVA coupled to oleoyl liposomes was processed beyond LAMP-1-expressing compartments (green spots), a portion of DQ-OVA was processed at compartments expressing LAMP-1 (yellow spots). Co-localization of EEA1-expressing compartments with liposome-coupled-DQ-OVA was significantly less than that of LAMP-1-expressing compartments with DQ-OVA (Fig. 4B).

T cell activation by APCs pulsed with liposomal antigen

In agreement with the results shown in Fig. 3, antigen presentation by APCs pulsed with liposomal antigen was significantly inhibited by DMA but not by cytochalasin B in both $CD4^+$- and $CD8^+$ T cell responses (Fig. 5).

Discussion

In general, extracellular antigens are presented via MHC class II molecules to $CD4^+$ T cells, whereas intracellular antigens are presented via MHC class I molecules to $CD8^+$ T cells. Consequently, most APCs do not present exogenous antigens via MHC class I since exogenous antigens do not gain access to the cytosolic compartment. Therefore, exogenous antigens usually do not prime CTL responses *in vivo*. This segregation of exogenous antigens from the class I pathway is important to prevent CTL from killing healthy cells that have been exposed to foreign antigens but are not infected [26]. However, there are several exceptions to this rule, reflecting the ability of the exogenous antigens to be delivered into the cytosolic compartments [13–17].

We have previously reported that antigens coupled to the surface of liposomes comprised of unsaturated fatty acid are presented to both $CD4^+$- and $CD8^+$ T cells [23]. Confocal laser scanning microscopic analysis demonstrated that a portion of the liposome-coupled antigens were taken up and processed beyond the MHC class II compartment. In the present study, we confirmed that OVA coupled to oleoyl liposomes was processed at both the MHC class I and class II compartments (Fig. 1). Flow cytometric analysis demonstrated that OVA coupled to oleoyl liposomes was incorporated more efficiently by macrophages than OVA coupled to stearoyl liposomes (Fig. 2). Furthermore, OVA coupled to oleoyl liposomes was taken up by macrophages even in a 4°C environment, in which antigen entry could only occur via plasma membrane translocation. In general, antigen processing pathways largely depend on the route of antigen uptake, and liposomes with a certain lipid component are known to fuse with the plasma membrane [27]. The uptake of OVA coupled to oleoyl liposomes in a 4°C environment observed in the present study suggested that oleoyl liposome might fuse with the plasma membrane and thereby allow the liposome-coupled antigen direct access to the cytosol. The role of endocytosis in the uptake of the liposomal antigen was further examined by using specific inhibitors for antigen uptake (Fig. 3). Cytochalasin B treatment of APCs prior to the addition of liposomal antigen in the culture had little effect. However, treatment of APCs with DMA significantly reduced the uptake of liposome-coupled OVA. Consequently, it was suggested that antigens coupled to oleoyl liposomes might be taken up by APCs via at least two pathways, penetration and pinocytosis. The analysis of intracellular pathways of antigens coupled to oleoyl liposomes using confocal laser scanning microscopy demonstrated that a portion of liposomal antigens taken up by APC were translocated to the lysosomal compartments expressing LAMP-1 (Fig. 4), suggesting that the liposomal antigens processed at lysosomal compartment and beyond lysosomal compartment might be presented to CD4/$CD8^+$ T cells via MHC class II and class I, respectively. In agreement with the results of antigen uptake shown in Fig. 3, the treatment of splenic $CD11c^+$ cells with DMA significantly reduced antigen presentation of liposomal antigens to both $CD4^+$- and $CD8^+$ T cells as evaluated by T-cell activation (Fig. 5).

It was reported that pinocytosis and scavenger receptor-mediated endocytosis by APC facilitate antigen presentation to $CD4^+$ T cells; by contrast, mannose receptor-mediated endocytosis by APC has been shown to facilitate antigen presentation to $CD8^+$ T cells [28]. However, as described in Materials and Methods, the oleoyl liposomes used in the present study do not contain mannose.

Thus, the data in the present study demonstrated that antigens coupled to oleoyl liposomes were internalized by APCs through both penetration and pinocytosis. The antigens coupled to the surface of oleoyl liposomes were processed at both MHC class I

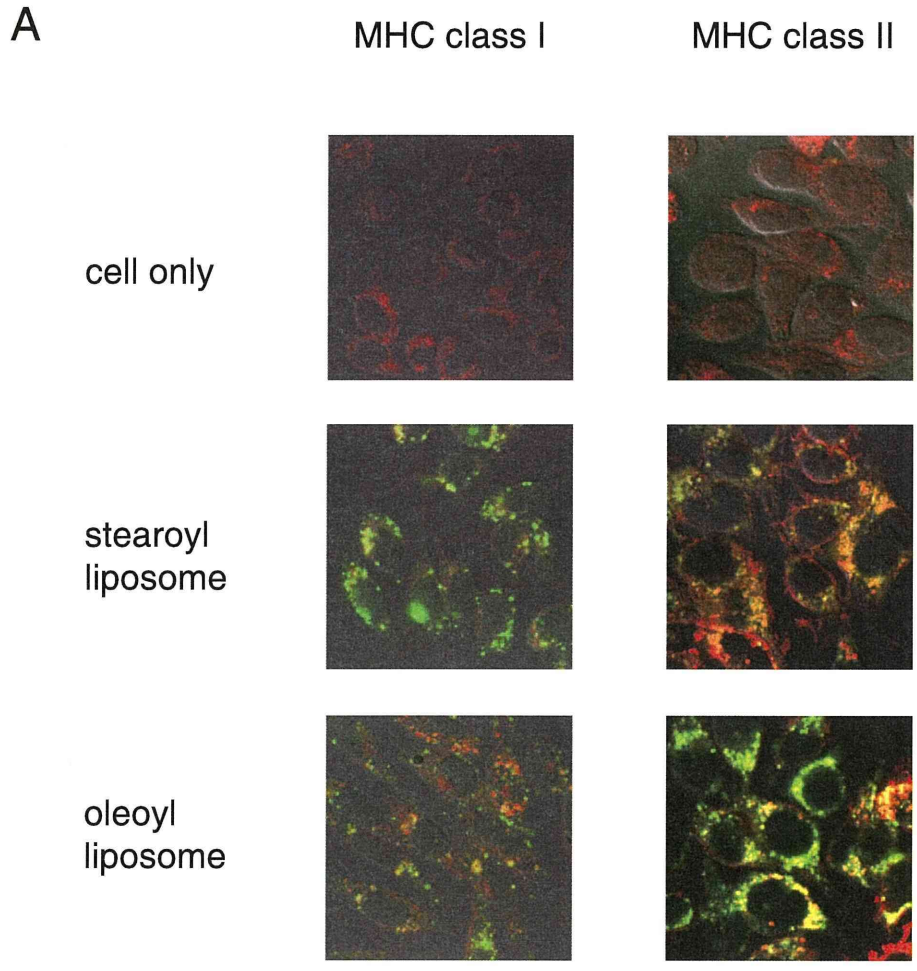
A
MHC class I
MHC class II
cell only
stearoyl liposome
oleoyl liposome

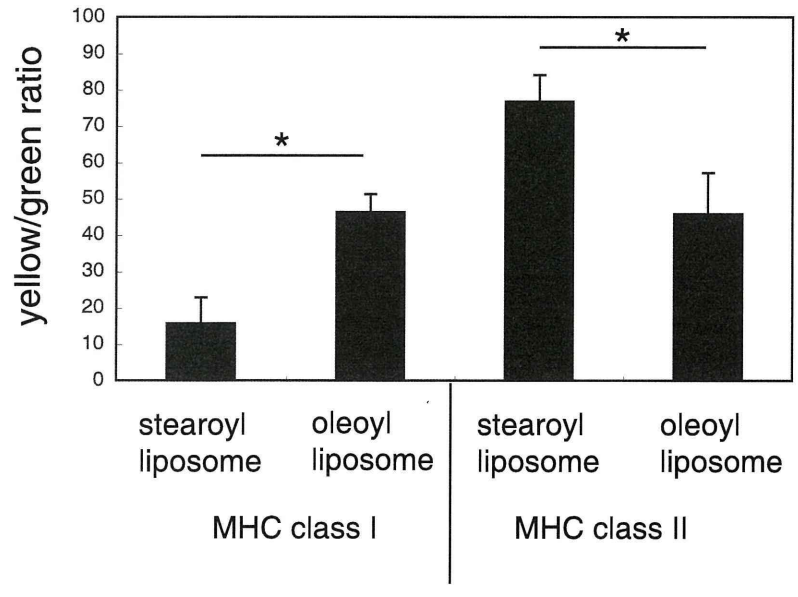
B
yellow/green ratio
100
90
80
70
60
50
40
30
20
10
0
*
*
stearoyl liposome
oleoyl liposome
stearoyl liposome
oleoyl liposome
MHC class I
MHC class II

Figure 1. Confocal laser scanning microscopic analysis of macrophages co-cultured with DQ-OVA-liposome conjugates. A, DQ-OVA was coupled to either stearoyl or oleoyl liposomes and added to the culture of cloned macrophages expressing DM-DsRed (class II) or labeled with red fluorescein (class I), as described in Materials and Methods. Two hours after the onset of the culture, macrophages were recovered and analyzed using confocal laser scanning microscopy. These optically merged images are representative of most cells examined by confocal microscopy. Yellow, co-localization of green (DQ-OVA after proteolytic degradation) and red (macrophage DM or class I); cell only, macrophages without co-culture with DQ-OVA-coupled liposomes. B, the green- and yellow-color compartments in the immunofluorescent pictures were quantified by the image analysis software MetaMorph, as described in Materials and Methods. Ratios of the yellow to green compartments are shown. Data represent the mean values ± SD of the images shown in Fig. 1A. Asterisk, significant ($p<0.01$) difference of samples.
doi:10.1371/journal.pone.0015225.g001

and class II compartments and presented to $CD4^+$- and $CD8^+$ T cells. Although the detailed pathway leading to presentation to both $CD4^+$- and $CD8^+$ T cells remains unclear, the observed behavior of antigens coupled to oleoyl liposome in APCs seems quite unique. Taken together, coupling of antigens to oleoyl liposome might potentially serve as a novel method to induce both humoral and cellular immunity.

Materials and Methods

Mice

CBF1 mice (8 weeks of age, female) were purchased from SLC (Shizuoka, Japan). All experiments were approved (No. 208021 and 209082) by an independent animal ethics committee at National Institute of Infectious Diseases, Tokyo, Japan.

Chemicals

All phospholipids were provided by NOF Co. (Tokyo, Japan). Reagent grades of cholesterol were purchased from Wako Pure Chemical (Osaka, Japan).

Antigens and reagents

Ovalbumin (OVA, Grade VII) was purchased from Sigma-Aldrich. For the analysis of the processing of liposome-coupled OVA by macrophages, DQ-OVA, which exhibits green fluores-

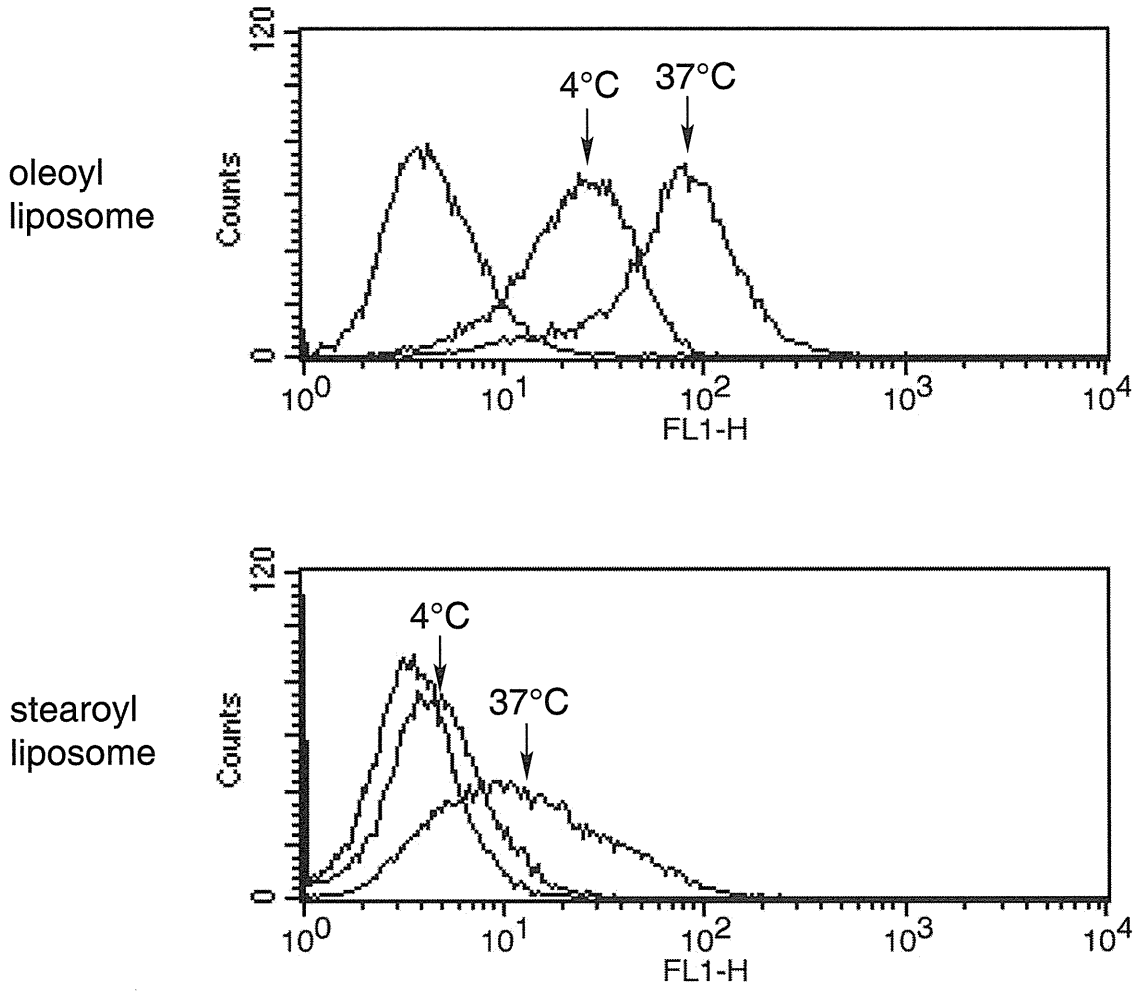

Figure 2. Uptake of liposome-coupled OVA by macrophages. Alexa-labeled OVA was coupled to either stearoyl or oleoyl liposomes and added to the culture of cloned macrophages as described in Materials and Methods. Thirty minutes after the onset of the culture, macrophages were recovered and analyzed using flow cytometry.
doi:10.1371/journal.pone.0015225.g002

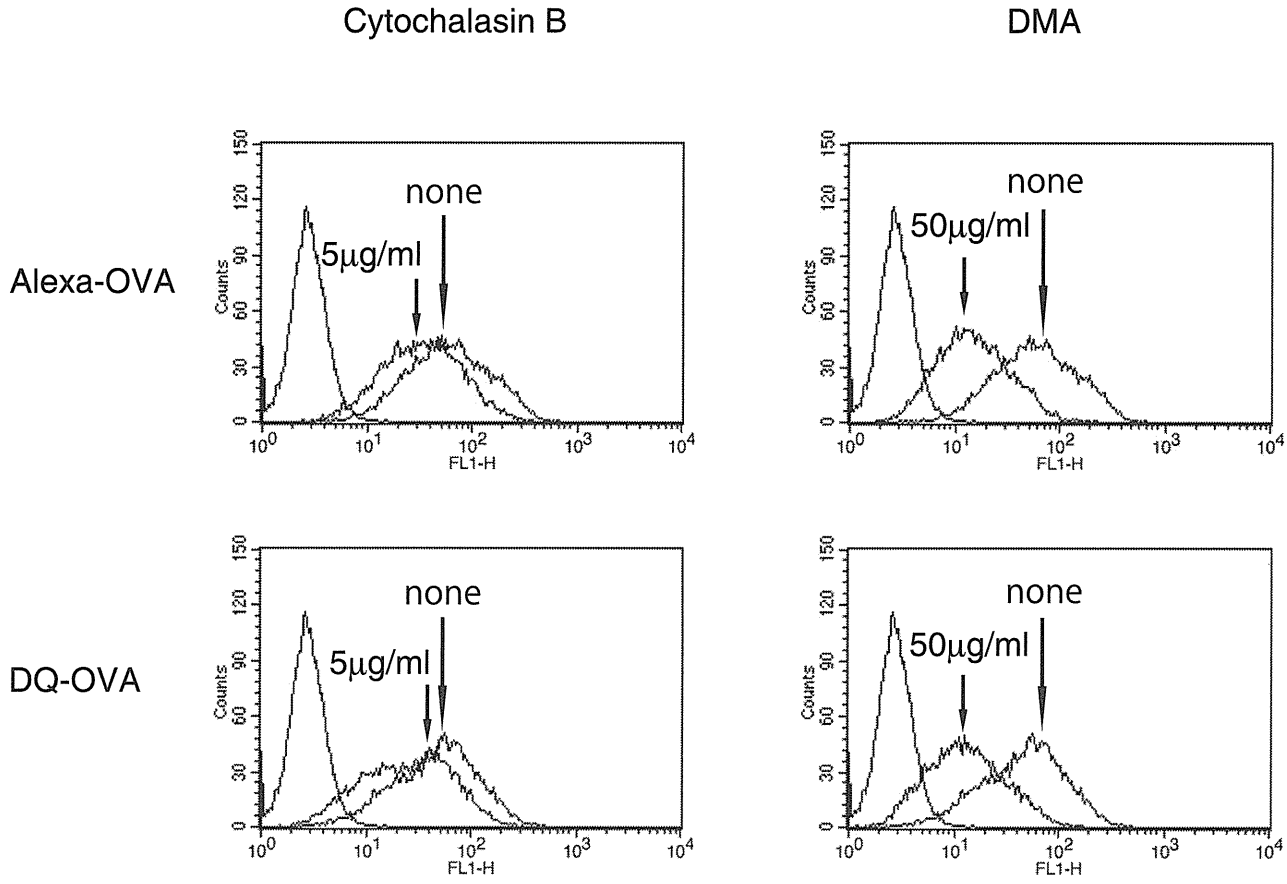

Figure 3. Influence of inhibitors for uptake of OVA coupled to oleoyl liposomes by macrophages. Alexa- or DQ-labeled OVA was coupled to oleoyl liposomes and added to the culture of macrophages as described in Materials and Methods. Treatment of macrophages with cytochalasin B or DMA was done 60 minutes prior to the addition of OVA-liposome conjugates.
doi:10.1371/journal.pone.0015225.g003

cence upon proteolytic degradation, was purchased from Molecular Probes, Inc. Synthetic CpG ODN (5002: TCCATGACGTTCTTGATGTT) was purchased from Invitrogen and was phosphorothioate-protected to avoid nuclease-dependent degradation.

Fluorescence labeling of OVA

OVA was labeled with fluorescence using an AlexaFluor 488 protein labeling kit (Invitrogen) according to the manufacturer's protocol.

Liposomes

Liposomes consisting of two different kinds of lipid were used in this study. Liposomes consisting of saturated fatty acids were composed of distearoyl phosphatidylcholine, distearoyl phosphatidyl ethanolamine, distearoyl phosphatidyl glycerol acid, and cholesterol in a 4:3:2:7 molar ratio (stearoyl liposomes), and liposomes consisting of unsaturated fatty acids were composed of dioleoyl phosphatidylcholine, dioleoyl phosphatidyl ethanolamine, dioleoyl phosphatidyl glycerol acid, and cholesterol in a 4:3:2:7 molar ratio (oleoyl liposomes). The crude liposome solution was passed through a membrane filter (nucleopore polycarbonate filter, Coster) with a pore size of 0.2 mm.

Coupling of OVA to liposomes

Liposomal conjugates with plain OVA, Alexa-labeled OVA, or DQ-OVA were prepared essentially in the same way as described previously [22]. Briefly, to a mixture of 90 mg of liposomes and 6 mg of OVA in 2.5 ml phosphate buffer (pH 7.2), 0.5 ml of 2.5% glutaraldehyde solution was added in dropwise fashion. The mixture was stirred gently for 1 h at 37°C, and then 0.5 ml of 3 M glycine-NaOH (pH 7.2) was added to block excess aldehyde groups. This was followed by incubation overnight at 4°C. The liposome-coupled OVA and uncoupled OVA in the resulting solution were separated using CL-4B column chromatography (Pharmacia). The amount of lipid in the liposomal fraction was measured using a phospholipid content assay kit (Wako Pure Chemical). The OVA-liposome solution was adjusted to 10 mg lipid/ml in PBS, sterile-filtered using a Millex-HA syringe filter unit (0.45 μm, Millipore), and kept at 4°C until use.

Quantification of OVA coupled to liposome

For the measurement of OVA coupled to liposome, radiolabeled OVA (*methyl*-^{14}C; purchased from New England Nuclear) was mixed with cold OVA and used for coupling with liposome and for determining the calibration curve. The

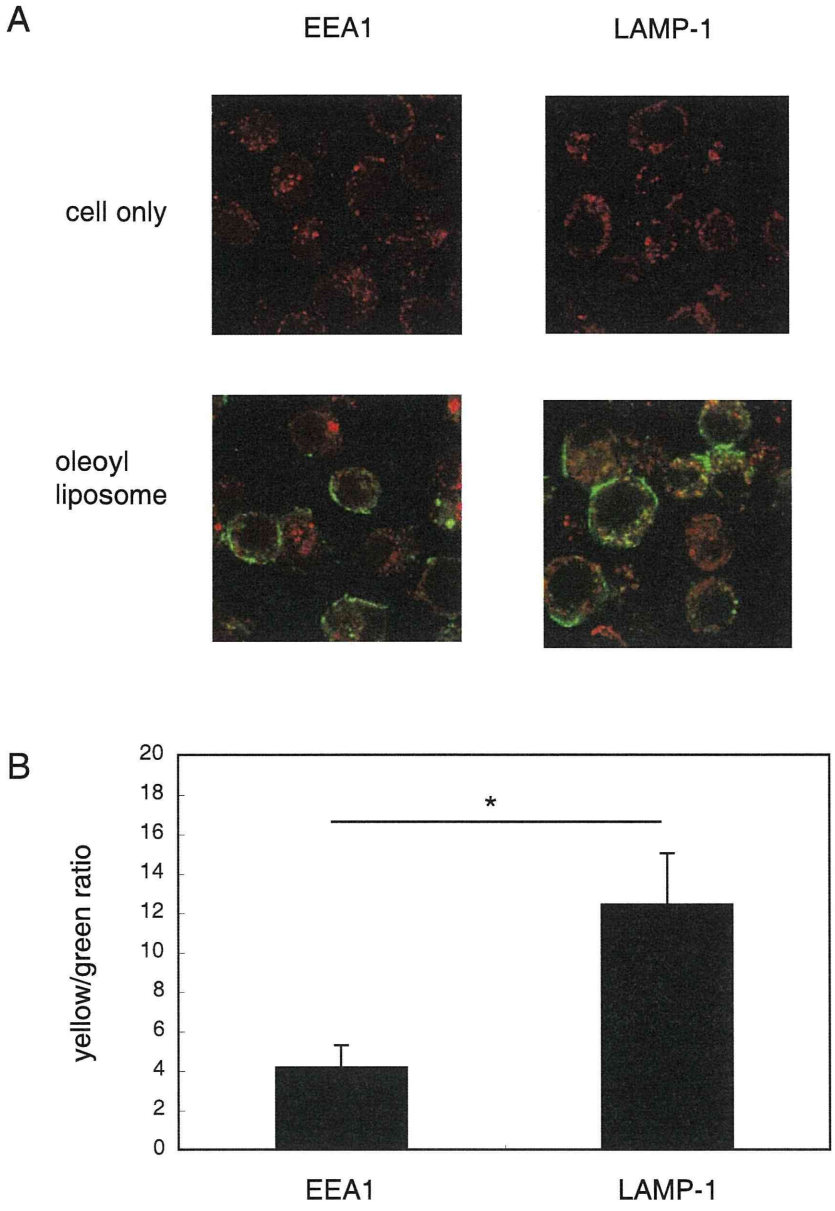

Figure 4. Intracellular localization of liposomal antigens taken up by macrophages. A, DQ-OVA was coupled to oleoyl liposomes and added to the culture of cloned macrophages of which endosomal marker EEA1-positive compartments, or lysosomal marker LAMP-1-positive compartments were stained as described in Materials and Methods. Two hours after the onset of the culture, macrophages were recovered and analyzed using confocal laser scanning microscopy. These optically merged images are representative of most cells examined by confocal microscopy. Yellow, co-localization of green (DQ-OVA after proteolytic degradation) and red (macrophage EEA1 or LAMP-1); cell only, macrophages without co-culture with DQ-OVA liposomes. B, the green- and yellow-color compartments in the immunofluorescent pictures were quantified by the image analysis software MetaMorph, as described in Materials and Methods. Ratios of the yellow to green compartments are shown. Data represent the mean values ± SD of the images shown in Fig, 4A. Asterisk, significant ($p<0.01$) difference of samples.
doi:10.1371/journal.pone.0015225.g004

radioactivity of the resulting OVA-liposome solution was counted using a calibration curve. The amounts of OVA coupled to stearoyl and oleoyl liposomes were 47.0 and 46.8 μg/mg lipid, respectively.

Immunization

Mice were immunized subcutaneously (s.c.) with the OVA-liposome conjugate at a dose of 1 mg lipid/100 μl/mouse in the presence of 5 μg/mouse CpG.

Cloned macrophage hybridoma

Macrophage hybridoma clone 39, obtained from the fusion of splenic adherent cells from CKB mice and P388D1 [29], was used.

Construction and expression of the fusion protein, DM-DsRed, in macrophage clone 39

The DNA fragment coding the full-length H2-DMβ2 [30] was amplified by PCR with two primers (5′-ATGGCTGCACT-CTGGCTGCTGCTGCTGGT-3′ and 5′-GATGCCGTCCT-

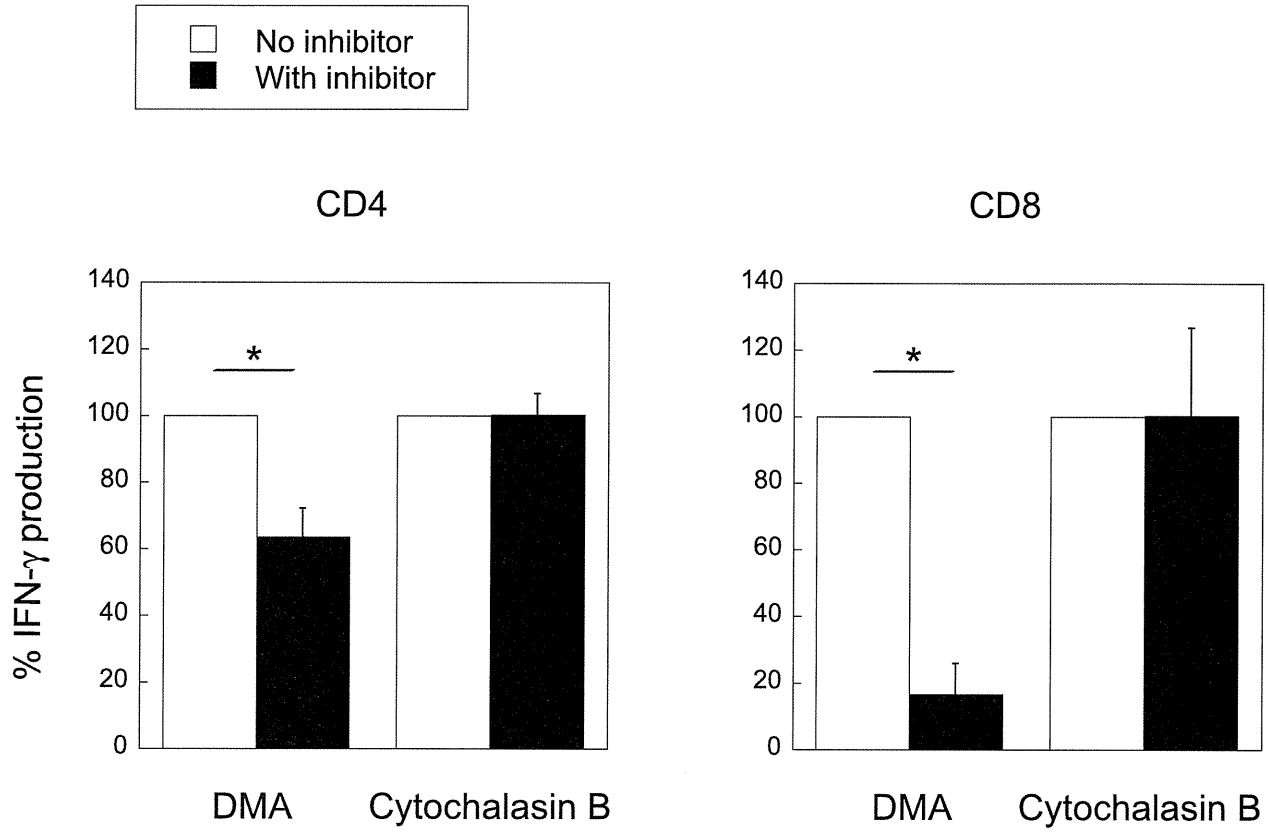

Figure 5. IFN-γ production by splenic CD4/CD8$^+$ T cells of mice immunized with OVA after co-culture with CD11c$^+$ cells pulsed with OVA coupled to oleoyl liposomes. Splenic CD4/CD8$^+$ T cells were taken from mice immunized with OVA and were cultured with CD11c$^+$ cells pulsed with OVA coupled to oleoyl liposomes with or without inhibitors as described in Materials and Methods. IFN-γ production of T cells in the supernatants in the absence of inhibitors was normalized to 100%. Data represent the mean values ± SD of triplicate culture. Asterisk, significant ($p<0.01$) difference as compared with the 'no inhibitor' group.
doi:10.1371/journal.pone.0015225.g005

TCTGGGTAGGTGGATCC-3′). The PCR product was cloned into the CMV promoter-driven expression plasmid pDsRedN1 (BD Clontech). This construct omitted the stop codon of H2-DMβ2 and encoded the H2-DMβ2 fused with DsRed. The cloned plasmid DNA was transfected to macrophage hybridoma clone 39 with Effectene transfection reagent (Qiagen) according to the manufacturer's protocol. During the transfection to clone 39, the medium containing cDNA and the transfection reagent was replaced with fresh medium after an 8-h transfection, and then clone 39 was cultured for 40 h. To obtain stable cell lines, clone 39 was passaged at 1:5 into RPMI 1640 containing 10% FCS with 50 μg/ml geneticin (G-418; Sigma-Aldrich). Cells showing the best fluorescence were selected using a FACS Vantage cell sorter (BD Bioscience). After cell sorting, clone 39 expressing DM-DsRed was cultured in RPMI 1640 containing 10% FCS with 200 μg/ml geneticin.

Flow cytometry

To investigate the capture of OVA-liposome conjugates by macrophages, macrophage clone 39 was incubated for 30 min at 4°C or 37°C in the presence of fluorescence-labeled OVA-liposome conjugates that contained a final concentration of 4 μg/ml OVA. After the incubation, cells were washed with ice-cold PBS. In the case of using Alexa-labeled OVA-liposome conjugates, cells were then incubated with 1.2 μg/ml trypan-blue for 5 min at 4°C to block the fluorescence of Alexa-OVA attached to the cell surface. After the cells were washed, they were analyzed on a FACS Caliber flow cytometer (BD Bioscience). The histograms of fluorescence distribution were plotted as the number of cells versus fluorescence intensity on a logarithmic scale.

Confocal laser scanning microscopy

To investigate the localization of OVA-liposome conjugates by macrophages, macrophage clone 39 or DM-DsRed-expressing cloned macrophage 39 was cultured for 18 h at 37°C on 8-hole heavy Teflon-coated slides (Bokusui Brown) and was then incubated with DQ-OVA-liposome conjugates, prepared using oleoyl or stearoyl liposomes, for 2 h at 37°C. The slides were then washed with MEM and fixed with 4% paraformaldehyde in PBS for 10 min at room temperature. After fixation, they were incubated for 10 min in 0.1 M glycine-HCl (pH 7.0) to block the remaining aldehyde residue. They were then washed two times in PBS. After washing, the slides were sealed with PBS:glycerin (1:9) and analyzed under an LSM510 confocal laser scanning microscope system (Zeiss). For analysis of co-localization of OVA and MHC class I, early endosomal antigen 1 (EEA1) or lysosomal-associated membrane protein-1 (LAMP-1) after blocking of the remaining aldehyde residue, cloned macrophage 39 was subsequently permeabilized with 0.05% saponin-TBS for 10 min at room temperature. After being washed twice with PBS, they were reacted with biotin-conjugated mouse anti-mouse H-2D^d mAb (34-2-12, 10 μg/ml; BD Biosciences), goat anti-mouse EEA1

polyclonal antibody (N19, 1 μg/ml; Santa Cruz Biotechnology) or rat anti-mouse LAMP-1 monoclonal antibody (1D4B, 1 μg/ml; Santa Cruz Biotechnology) for 18 h at 4°C. After being washed three times with TBS, they were reacted with Alexa 546-conjugated streptavidin (1:200 diluted; Invitorogen) to detect MHC class I, Alexa Fluor 568-labeled Ab (rabbit anti-goat IgG, 10 μg/ml; Invitrogen) to detect EEA1 or Alexa Fluor 568-labeled Ab (goat anti-rat IgG, 10 μg/ml; Invitrogen) to detect LAMP-1 for 4 h at room temperature. They were then washed two times in TBS. After the washing, the slides were sealed with PBS:glycerin (1:9) and analyzed under an LSM510 confocal laser scanning microscope system (Zeiss).

Quantification of immunofluorescent pictures and statistics

Quantification of confocal image analysis was done by single cell identification using the image analysis software MetaMorph (Molecular Devices Co., Tokyo, Japan), and the relative fluorescence intensity of green, red, and yellow pixels was assessed. The relative fluorescence intensity of all individual colors was then expressed as percent of the total fluorescence intensity. *p* values were calculated by the Student's t test with two-tailed distribution and two-sample unequal variance parameters.

Inhibition Studies of Antigen Uptake

In the case of inhibition studies, cloned macrophage 39 or $CD11c^+$ cells were incubated with indicated inhibitors 60 min before and throughout the antigen pulse. Cytochalasin B [31] and DMA [28] were purchased from Sigma.

Preparation of $CD11c^+$ cells and $CD4^+$- and $CD8^+$ T cells

$CD11c^+$ spleen cells of naïve mice and $CD4^+$ T and $CD8^+$ T spleen cells of mice immunized with OVA-liposome conjugates were prepared with the magnetic cell sorter system MACS, according to the manufacturer's protocol using anti-CD11c, anti-CD4 and anti-CD8 antibody-coated microbeads (Miltenyi Biotec).

Culture of $CD4^+$- and $CD8^+$ T cells with $CD11c^+$ cells pulsed with OVA

$CD11c^+$ cells were incubated with or without the indicated inhibitors for 60 min in a 24-well plate prior to the addition of OVA-liposome conjugates made using oleoyl liposomes. The final concentration of OVA-liposome added to the macrophage culture was 500 μg lipid/ml, which included 24 μg OVA. After 60 minutes' incubation, $CD11c^+$ cells were washed 3 times in ice-cold medium and 2×10^5 cells were co-cultured with 5×10^5 $CD4^+$ T cells or $CD8^+$ T cells, in a 48-well plate. A preliminary experiment showed that the optimal culture period in the above culture condition was 2 days for IFN-γ production by $CD4^+$ T cells and 5 days for IFN-γ production by $CD8^+$ T cells. After incubation in a CO_2 incubator for 2 or 5 days, the culture supernatants were collected and assayed for IFN-γ.

IFN-γ Assay

IFN-γ in the culture supernatants was measured using the Biotrak mouse ELISA system (GE Healthcare). All test samples were assayed in duplicate, and the SD in each test was always $<5\%$ of the mean value.

Author Contributions

Conceived and designed the experiments: MT TU. Performed the experiments: YT MT TK TU. Analyzed the data: MT MK TU. Contributed reagents/materials/analysis tools: MT TU. Wrote the paper: MT TU.

References

1. Mark A, Björkstén B, Granstörm M (1995) Immunoglobulin E responses to diphtheria and tetanus toxoids after booster with aluminium-adsorbed and fluid DT-vaccines. Vaccine 13: 669–673.
2. Aggerbeck H, Wantzin J, Heron I (1996) Booster vaccination against diphtheria and tetanus in man. Comparison of three different vaccine formulations – III. Vaccine 14: 1265–1272.
3. Nothdurft HD, Jelinek T, Marschang A, Maiwald H, Kapaun A, et al. (1996) Adverse reactions to Japanese encephalitis vaccine in travelers. J Infect 32: 119–122.
4. Doherty PC, Kelso A (2008) Toward a broadly protective influenza vaccine. J Clin. Invest 118: 3273–3275.
5. McMichael AJ, Hanke T (2003) HIV vaccines 1983-2003. Nat. Med 9: 874–880.
6. Chen M, Sallberg M, Sonnerberg A, Weiland L, Mattsson L, et al. (1999) Limited humoral immunity in hepatitis C virus infection. Gastroenterology 116: 135–143.
7. Yerly D, Heckerman D, Allen TM, Chsiholm JV, III, Faircloth K, et al. (2008) Increased cytotoxic T-lymphocyte epitope variant cross-recognition and functional avidity are associated with hepatitis C virus clearance. J Virol 82: 3147–3153.
8. Bevan MJ (1987) Antigen recognition. Class discrimination in the world of immunology. Nature 325: 192–194.
9. Germain RN, Margulies DH (1993) The biochemistry and cell biology of antigen processing and presentation. Annu Rev Immunol 11: 403–450.
10. Norbury CC, Hewlett LJ, Prescott AR, Shastri N, Watts C (1995) Class I MHC presentation of exogenous soluble antigen via macropinocytosis in bone marrow macrophages. Immunity 3: 783–791.
11. Nelson D, Bundell C, Robinson B (2000) In Vivo Cross-presentation of a soluble protein antigen: kinetics, distribution, and generation of effect CTL recognizing dominant and subdominant epitopes. J Immunol 165: 6123–6132.
12. Chen W, Masterman K-A, Basta S, Haeryfer SMM, Dimopoulos N, et al. (2004) Cross-priming of $CD8^+$ T cells by viral and tumor antigens is a robust phenomenon. Eur J Immunol 34: 194–199.
13. Bevan MJ (1976) Cross-priming for a secondary cytotoxic response to minor H antigens with *H-2* congenic cells which do not cross-react in the cytotoxic assay. J Exp Med 143: 1283–1288.
14. Bevan MJ (2006) Cross-priming, Nat Immunol 7: 363–365.
15. Vyas JM, Veen AGVD, Ploegh HL (2008) The known unknown of antigen processing and presentation, Nature Rev Immunol 8: 607–618.
16. Kasturi SP, Pulendran B (2008) Cross-presentation: avoiding trafficking chaos? Nat Immunol 9: 461–463.
17. Rock KL (2003) The ins and outs of cross-presentation. Nat Immunol 4: 941–943.
18. Bankowski MK, Rock KL (1995) A phagosome-to-cytosol pathway for exogenous antigens presented on MHC class I molecules. Science 267: 243–246.
19. Rodriguez A, Regnault A, Kleijmeer M, Ricciardi-Castagnoli P, Amigorena S (1999) Selective transport of internalized antigens to cytosol for MHC class I presentation in dendritic cells. Nat Cell Biol 1: 362–368.
20. Shen L, Sigal LJ, Boes M, Rock KL (2004) Important role of cathepsin S in generating peptides for TAP-independent MHC class I crosspresentation in vivo. Immunity 21: 155–165.
21. Naito S, Horino A, Nakayama M, Nakano Y, Nagai T, et al. (1996) Ovalbumin-liposome conjugate induces IgG but not IgE antibody production. Int Arch Allergy Immunol 109: 223–228.
22. Nakano Y, Mori M, Nishinohara S, Takita Y, Naito S, et al. (1999) Antigen-specific, IgE-selective unresponsiveness induced by antigen-liposome conjugates. Comparison of four different conjugation methods for the couplong of antigen to liposome. Int Arch Allergy Immunol 120: 199–208.
23. Taneichi M, Ishida H, Kajino K, Ogasawara K, Tanaka Y, et al. (2006) Antigen chemically coupled to the surface of liposomes are cross-presented to $CD8^+$ T cells and induce potent antitumor immunity. J Immunol 177: 2324–2330.
24. Ohno S, Kohyama S, Taneichi M, Moriya O, Hayashi H, et al. (2009) Synthetic peptides coupled to the surface of liposomes effectively induce SARS coronavirus-specific cytotoxic T lymphocytes and viral clearance in HLA-A*0201 transgenic mice, Vaccine 27: 3912–3920.
25. Matsui M, Kohyama S, Suda S, Yokoyama S, Mori M, et al. (2010) A CTL-based liposomal vaccine capable of inducing protection against heterosubtypic influenza viruses in HLA-A*0201 transgenic mice. Biochem Biophys Res Commun 391: 1494–1499.
26. Rock KL (2006) Exiting the outside world for cross-presentation. Immunity 25: 523–525.
27. Felgner PL, Gadek TR, Holm M, Roman R, Chan HW, et al. (1987) Lipofection: a highly efficient, lipid-mediated DNA-transfection procedure. Proc. Natl Acad Sci USA 84: 7413–7417.

28. Burgdorf S, Kautz A, Böhnert V, Knolle PA, Kurts C (2007) Distinct pathways of antigen uptake and intracellular routing in CD4 and CD8 T cell activation. Science 316: 612–616.
29. Uchida T, Ju S, Fay A, Liu Y, Dorf ME (1985) Functional analysis of macrophage hybridomas. I. Production and initial characterization. J Immunol 134: 772–778.
30. Hermel E, Yuan J, Monaco JJ (1995) Characterization of polymorphism within the H2-M MHC class II loci. Immunogenetics 42: 136–142.
31. Gurnani K, Kennedy J, Sad S, Sprott GD, Krishnan L (2004) Phosphatidylserine receptor-mediated recognition of archaeosome adjuvant promotes endocytosis and MHC class I cross-presentation of the entrapped antigen by phagosome-to-cytosol transport and classical processing. J Immunol 173: 566–578.

frontiers in
MICROBIOLOGY

ORIGINAL RESEARCH ARTICLE
published: xx November 2010
doi: 10.3389/fmicb.2010.00128

Characterization of natural killer cells in tamarins: a technical basis for studies of innate immunity

Tomoyuki Yoshida[1,2†], Akatsuki Saito[2,3†], Yuki Iwasaki[1,4], Sayuki Iijima[1], Terue Kurosawa[1], Yuko Katakai[5], Yasuhiro Yasutomi[6], Keith A. Reimann[7], Toshiyuki Hayakawa[2] and Hirofumi Akari[1,2]*

[1] *Tsukuba Primate Research Center, National Institute of Biomedical Innovation, Tsukuba, Ibaraki, Japan*
[2] *Primate Research Institute, Kyoto University, Inuyama, Aichi, Japan*
[3] *International Research Center for Infectious Diseases, The Institute of Medical Science, The University of Tokyo, Minato-ku, Tokyo, Japan*
[4] *Graduate School of Medicine and Dentistry, Tokyo Medical and Dental University, Bunkyo-ku, Tokyo, Japan*
[5] *Corporation for Production and Research of Laboratory Primates, Tsukuba, Ibaraki, Japan*
[6] *Laboratory of Immunoregulation and Vaccine Research, Tsukuba Primate Research Center, National Institute of Biomedical Innovation, Tsukuba, Ibaraki, Japan*
[7] *Division of Viral Pathogenesis, Beth Israel Deaconess Medical Center, Harvard Medical School, Boston, MA, USA*

Edited by:
Yasuko Yokota, National Institute of Infectious Diseases, Japan

Reviewed by:
Koji Ishii, National Institute of Infectious Diseases, Japan
Ikuo Shoji, Kobe University Graduate School of Medicine, Japan

***Correspondence:**
Hirofumi Akari, Primate Research Institute, Kyoto University, Inuyama, Aichi 484-8506, Japan.
e-mail: akari@pri.kyoto-u.ac.jp

†*Tomoyuki Yoshida and Akatsuki Saito have contributed equally to this work.*

Natural killer (NK) cells are capable of regulating viral infection without major histocompatibility complex restriction. Hepatitis C is caused by chronic infection with hepatitis C virus (HCV), and impaired activity of NK cells may contribute to the control of the disease progression, although the involvement of NK cells *in vivo* remains to be proven. GB virus B (GBV-B), which is genetically most closely related to HCV, induces acute and chronic hepatitis upon experimental infection of tamarins. This non-human primate model seems likely to be useful for unveiling the roles of NK cells *in vivo*. Here we characterized the biological phenotypes of NK cells in tamarins and found that depletion of the $CD16^+$ subset *in vivo* by administration of a monoclonal antibody significantly reduced the number and activity of NK cells.

Keywords: CD16, cynomolgus monkey, tamarin, NK cell

INTRODUCTION

Natural killer (NK) cells are a component of the innate immune system that play a central role in host defense against viral infection and tumor cells. Much of the evidence for a role for NK cells in controlling viral infections has come from experiments with mice that were genetically modified (Lian and Kumar, 2002) or were treated with NK cell-depleting antibodies (Kasai et al., 1980) or from the study of humans with inherited NK cell deficiencies (Biron et al., 1989; Orange, 2002).

NK cells can be rapidly recruited into infected organs and tissue by chemoattractant factors produced by virus-infected cells and activated resident macrophages, which are also a major source of interferon (IFN), which induces NK cell proliferation, NK cell-mediated cytolysis of virus-infected cells, and the secretion of chemokines (Robertson, 2002). NK cells can kill virus-infected cells by using cytotoxic granules or by recognizing and inducing lysis of antibody-coated target cells (antibody-dependent cell cytotoxicity) via antibody binding receptor CD16. For instance, human blood NK cells are cytotoxic against dengue virus-infected cells in target organs via direct cytolysis and antibody-dependent cell-mediated cytotoxicity (reviewed by Navarro-Sánches et al., 2005). Early activity of NK cells may be important for clearing acute infections such as that of dengue virus. However, the effect that NK cells may exert on chronic infections with viruses such as hepatitis C virus (HCV) is less clear.

HCV is the causative agent of chronic hepatitis C, cirrhosis, and finally liver cancer. In general, acquired and innate immunity induced by acute HCV infection is not sufficient for the viral clearance, and persistent HCV infection frequently leads to progression to chronic hepatitis (reviewed by Cheent and Khakoo, 2010). It was reported that dendritic cells (DCs) in HCV infection were not responsive to IFN-α, and thus failed to promote subsequent activation of NK cells as a primary innate immune response (reviewed by Kanto, 2008). This is in agreement with the finding that the killing activity of NK cells in patients with chronic hepatitis C is inactivated in *in vitro* studies (Deignan et al., 2002; Golden-Mason et al., 2008). These data suggest that the dysfunction of NK cells contributes to the persistent infection of HCV and chronic hepatitis. On the other hand, it was suggested that inappropriately activated NK cells caused liver injury after the viral infection (Liu et al., 2000). The population of NK cells is relatively minor in peripheral lymphoid organs but is abundant in liver, raising a question as to their function in the innate immune response to acute and chronic HCV infection in the liver. It is possible that NK cells partially regulate the replication of HCV in this organ during early infection whereas they promote the liver dysfunction in chronic HCV infection. To examine these possibilities, it is necessary to clarify the involvement of NK cells *in vivo* in HCV infection. However, it is questionable whether the results of *ex vivo* analyses of NK cells would reflect their actual roles *in vivo*. Therefore, it might be more informative to study the function of NK cells directly by means of *in vivo* depletion technique in animal models.

A chimpanzee model of HCV infection has frequently been employed to evaluate the role of acquired antiviral immune responses, although the involvement of NK cells has not been fully evaluated because of the limitations on the use of chimpanzees

due to ethical and financial restrictions (Cohen and Lester, 2007). Accordingly, New World monkeys infected with GB virus B (GBV-B) appear to be a promising model because (i) among viruses so far known, GBV-B is genetically the most closely related to HCV and can infect New World monkeys, including tamarins, marmosets and owl monkeys, but not Old World monkeys (reviewed by Akari et al., 2009), (ii) tamarins develop acute and chronic hepatitis after experimental GBV-B infection (Bukh et al., 1999; Sbardellati et al., 2001; Lanford et al., 2003; Martin et al., 2003; Ishii et al., 2007; Takikawa et al., 2010), (iii) the infection induces antiviral cellular immune responses (Woollard et al., 2008), and (iv) tamarins and marmosets are commercially available and easily handled, reared and bred. Moreover, tamarins, being primates, may have a similar immune system to humans, and therefore they may be useful for studying the function of NK cells against the hepatitis virus in this tamarin model.

Our final goal is to study the role of NK cells as a major player in innate immunity during the course of the progression of viral hepatitis. Since some basic information regarding the biological characteristics of NK cells still remains unclear, we initially sought to characterize NK cells in tamarins to provide a technical basis for further studies.

MATERIALS AND METHODS

ANIMALS

Five red-handed tamarins (*Saguinus midas*) and five cynomolgus monkeys (*Macaca fascicularis*) were used in this study. The animals were cared for in accordance with National Institute of Biomedical Innovation rules and guidelines for experimental animal welfare, and all protocols were approved by our Institutional Animal Study Committee.

FLOW CYTOMETRY

Flow cytometry was performed as previously described (Akari et al., 1997) with a slight modification. Fifty microliters of whole blood from cynomolgus monkeys and tamarins was stained with combinations of fluorescence-conjugated monoclonal antibodies (mAb): anti-CD3 (SP34-2; Becton Dickinson), anti-CD4 (L200; BD Pharmingen), anti-CD8 (CLB-T8/4H8; Sanquin), anti-CD16 (3G8; BD Pharmingen), and anti-CD16 (DJ130c; Dako). Then, erythrocytes were lysed with FACS lysing solution (Becton Dickinson). After having been washed with sample buffer containing phosphate-buffered saline (PBS), 1% fetal calf serum (FCS), and 1% formaldehyde, the labeled cells were resuspended in the sample buffer. The expression of the immunolabeled molecules on the lymphocytes was analyzed with a FACSCanto II flow cytometer (Becton Dickinson). Peripheral blood mononuclear cells (PBMCs) were separated from the blood of these monkeys by a Ficoll-Paque gradient method. The cells were resuspended in complete medium composed of RPMI-1640 medium supplemented with 10% FCS, 1% penicillin/streptomycin, 2 mM HEPES and 55 μM 2-mercaptoethanol at 4°C until use. Fluorochrome-labeled mouse mAbs were reacted with 2×10^5 PBMCs at 4°C for 30 min. The labeled cells were washed with PBS containing 1% FCS, and resuspended in the sample buffer. The expression of the immunolabeled molecules on the lymphocytes was analyzed as mentioned above.

FLOW CYTOMETRIC 5-(AND 6)-CARBOXYFLUORESCEIN DIACETATE SUCCINIMIDYL ESTER (CFSE)/7-AMINO ACTINOMYCIN D (7-AAD) CYTOTOXIC ASSAY

Peripheral blood mononuclear cells were separated from the blood of these monkeys by a Ficoll-Paque gradient method. These PBMCs were then resuspended in complete medium at 37°C until use. The flow cytometric CFSE/7-AAD cytotoxicity assay was performed as previously described (Lecoeur et al., 2001) with slight modifications. K562 cells (3×10^6) were labeled with 500 nM CFSE (from a 1 mM stock solution in dimethyl sulfoxide [Sigma] stored at −20°C) in Hanks' Balanced Salt Solution for 8 min at 37°C in total of 2 ml. The cells were then washed twice in complete medium and used immediately for the cytotoxicity assay. The CFSE-labeled target cells (20,000 cells) were used at different E (effector):T (target) ratios (0:1, 3:1, and 9:1). After 24 h incubation, the cells were stained with 0.25 μg/ml of 7-AAD and incubated for 10 min at 37°C in a CO_2 incubator. The cells were washed twice with 1% FCS–PBS, resuspended in sample buffer and analyzed immediately by flow cytometry.

MAGNETIC CELL SEPARATION

Magnetic cell separation (MACS) was performed as previously described (Tenorio and Saavedra, 2005) with slight modifications. PBMCs (1×10^7) were washed with 3 ml of MACS buffer composed of PBS with 2 mM EDTA and 0.5% bovine serum albumin, and resuspended in 100 μl of the same buffer. Ten microliters of fluorescein isothiocyanate (FITC)-labeled anti-CD16 mAb (3G8) was added. The cells with or without the mAb were incubated for 10 min at 4°C, washed with 1 ml of MACS buffer, and resuspended in 80 μl of the same buffer. They were mixed with 20 μl of anti-FITC MicroBeads and incubated for 15 min at 4°C, washed with 1 ml of MACS buffer, and resuspended in 500 μl of the same buffer. The CD16-positive cells were separated by negative selection using LD columns and a MACS separation unit following the instructions provided by the manufacturer (Miltenyi Biotec). CD16-negative cells were resuspended in complete medium and co-cultured with K562 cells at 37°C for the NK cytotoxicity assay immediately.

DETECTION OF CIRCULATING ANTI-CD16 MAB (3G8)

Concentrations of an anti-CD16 antibody (3G8) in plasma samples were assessed using a mouse IgG_1 Quantitative ELISA Kit (Bethye Laboratory, Inc.). The assay was performed according to the manufacturer's instruction with a slight modification. To detect the mAb in monkey plasma, 96-well enzyme-linked immunosorbent assay (ELISA) plates were coated with a capture antibody and incubated for 1 h at 37°C and washed with wash solution (50 mM Tris, 0.14 M NaCl, 0.05% Tween 20, pH 8.0) three times. The plates were blocked with blocking solution (Postcoat) for 30 min at 37°C. Plasma samples from antibody-treated monkeys were diluted in dilution buffer (50 mM Tris, 0.14 M NaCl, 1% bovine serum albumin, 0.05% Tween 20, pH 8.0), applied to the wells in serial dilutions, incubated for 1 h at 37°C and washed with the wash solution five times. Goat anti-mouse IgG_1 conjugated with horseradish peroxidase and diluted 1:50000 in dilution buffer was added to each well and incubated for 1 h at 37°C. Each well was washed with the wash solution five times. Substrate solution was added to each well and incubated

for 10–15 min at room temperature, and then the reaction was stopped with H_2SO_4. Optical density was measured using an ELISA reader at 450 nm.

IN VIVO DEPLETION OF CD16 POSITIVE CELLS

Mouse anti-human CD16 (3G8) mAb (Fleit et al., 1982) was produced in serum-free medium and purified using protein A affinity chromatography. Endotoxin levels were lower than 1 EU/mg. The antibody was administered to tamarins (Tm 05-003, Tm 06-020) and cynomolgus monkeys (Mf 00-005, Mf 99-110) intravenously at 50 mg/kg at a rate of 18 ml/min using a syringe pump. Lymphocyte subsets were monitored for 3 weeks after the administration.

STATISTICAL ANALYSIS

Statistical analyses of lymphocyte ratios were performed using Student's *t*-test and single-factor ANOVA, followed by Fisher's protected least-significant difference *post hoc* test by using StatView software (SAS Institute, NC, USA). The results were confirmed in more than three independent experiments in tamarins and cynomolgus monkeys.

RESULTS

LYMPHOCYTE SUBSETS IN TAMARINS

First, we examined the lymphocyte subsets in tamarins as compared with cynomolgus monkeys (**Figure 1**). The percentages of T and B lymphocytes indicated as $CD20^-CD3^+$ and $CD20^+CD3^-$ subsets in the total lymphocytes were found to be 68.8% (range 41.9–68.8%) and 12.3% (range 11.8–12.6%) in tamarins and 68.4% (range 42.6–68.4%) and 10.2% (range 9.1–11.4%) in cynomolgus monkeys, respectively. The percentage of $CD4^+$ T cells in the $CD3^+$ subset was 45.5% (range 41.9–52.5%) and 55.3% (range 42.6–64.4%) while that of $CD8^+$ T cells was 41.0% (range 35.8–44.5%) and 31.2% (range 29.3–34.6%) in tamarins and cynomolgus monkeys, respectively. Next, the NK cell subset was determined as $CD3^-$ $CD16^+$ lymphocytes in this study. The percentage of NK cells was 30.5% (range 16.9–52.5%) and 18.9% (range 13.7–22.4%) in tamarins and cynomolgus monkeys, respectively. We analyzed statistically whether these lymphocyte ratios were different between tamarins and cynomolgus monkeys, and found that there were no significant differences of the lymphocyte ratios between them. We therefore concluded that the proportions of the major lymphocyte subsets in tamarins were relatively similar to those in cynomolgus monkeys.

FLUORESCENCE-BASED *IN VITRO* ASSAY FOR QUANTITATIVELY EVALUATING NATURAL KILLER ACTIVITY

Natural killer cell cytotoxic assays conventionally require considerable numbers of PBMCs, and this has been a major hurdle for analyzing the NK activity in small New World monkeys due to the limited availability of their blood. Therefore, we employed an alternative method using a fluorescence-based assay to assess the activity of NK cells in tamarins as previously described (Lecoeur et al., 2001) with slight modifications. When CFSE-stained K562 target cells were incubated with the effector PBMCs obtained from tamarins at an effector/target (E/T) ratio of 9:1, 42% of the K562 cells were positive for 7-AAD, which stains apoptotic cells (**Figure 2A**). We

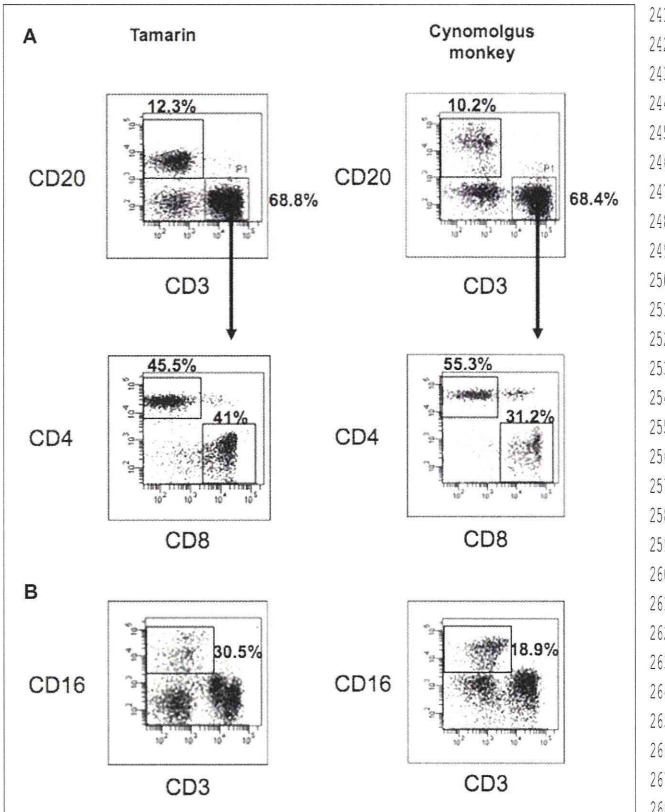

FIGURE 1 | Flow cytometric analysis of CD3, CD20, CD4, CD8, and CD16 expression on lymphocytes in cynomolgus monkeys and tamarins. Representative results in tamarins and cynomolgus monkeys are shown. **(A)** Flow cytometric analysis of CD3 and CD20 expression in lymphocytes (top panels) and CD4 and CD8 expression in $CD3^+$ population (bottom panels) of both monkeys. **(B)** Flow cytometric analysis of CD3 and CD16 expression in both monkey species. The numbers denote the percentages of lymphocytes. We analyzed statistically whether these lymphocyte ratios were different between tamarins and cynomolgus monkeys by using StatView software. There were no significant differences of the lymphocyte ratios between them.

confirmed that the killing activity of NK cells was dose-dependent, and that the level in tamarins was higher than that in cynomolgus monkeys (**Figures 2B and 3**).

Next, in order to examine if $CD16^+$ lymphocytes represent a major population with NK activity, $CD16^-$ PBMCs were obtained by negative selection using MACS (**Figure 4A**) in both tamarins and cynomolgus monkeys. We found that depletion of $CD16^+$ cells greatly attenuated the killing activity in both tamarins and cynomolgus monkeys (**Figure 4B**), indicating that $CD16^+$ lymphocytes are a major population with NK activity.

IN VIVO DEPLETION OF $CD16^+$ NK CELLS USING A MURINE ANTI-CD16 MAB

We next sought to establish a system to directly evaluate the role of NK cells in tamarins. We asked if the administration of an anti-CD16 (3G8) mAb could deplete $CD16^+$ lymphocytes *in vivo*. Tamarins were intravenously administered 3G8 or control mAb (MOPC-21) at a dose of 50 mg/kg. Using an anti-CD16 antibody that is not cross-blocked by 3G8 (clone DJ130c), it was found that at

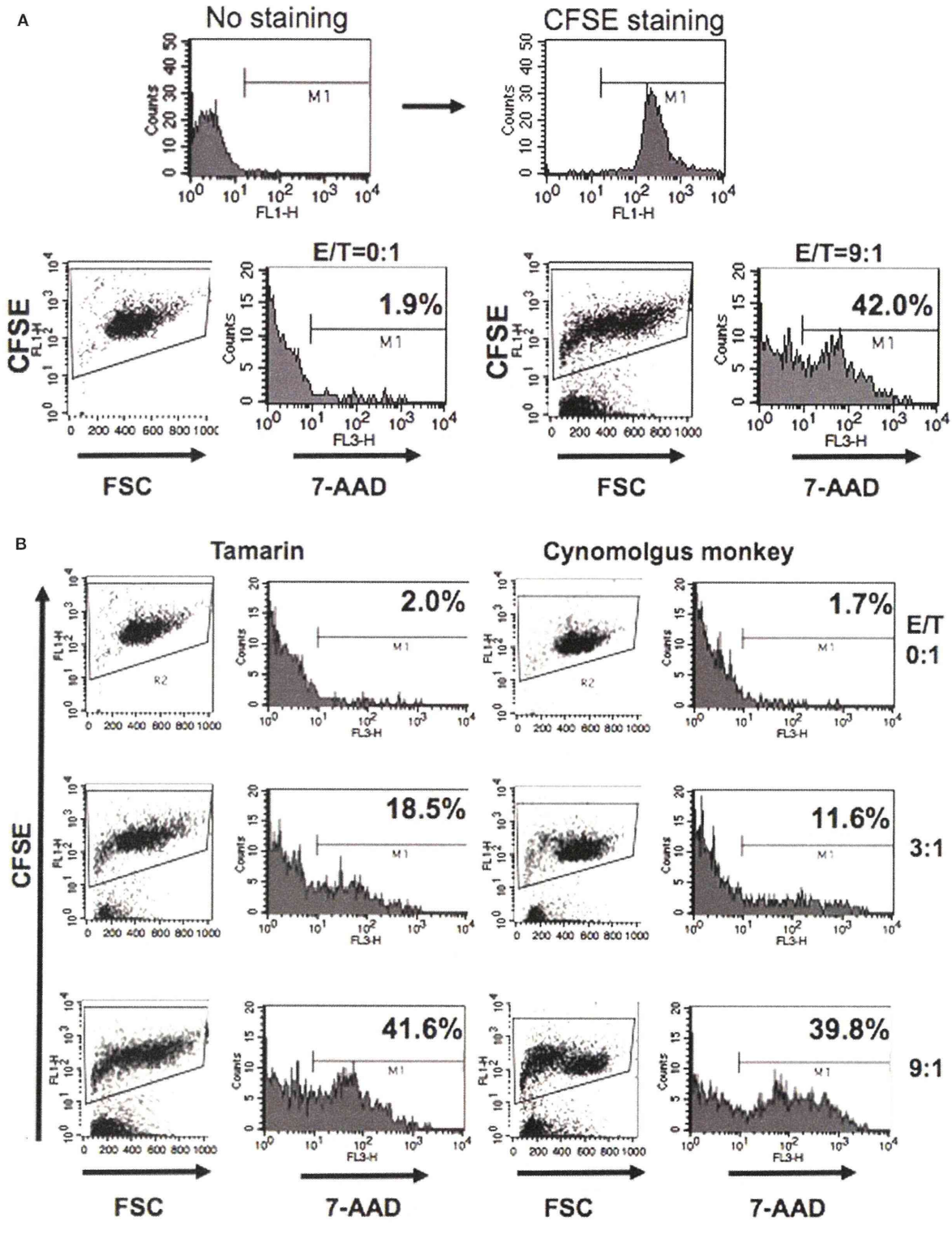

FIGURE 2 | Cytotoxicity assay by CFSE and 7-AAD staining. (A) CFSE-stained K562 cells were co-cultured with PBMCs at E/T ratios of 9:1 and 0:1. The CFSE-stained K562 cells were first gated by FSC and SSC characteristics, and 3000 events were captured. **(B)** CFSE-stained K562 target cells were killed by tamarin PBMCs using E/T ratios of 9:1, 3:1, and 0:1. The numbers in the panels denoted the percentages of 7-AAD positive cells. We analyzed statistically whether these killing activities were different between tamarins and cynomolgus monkeys by using StatView software.

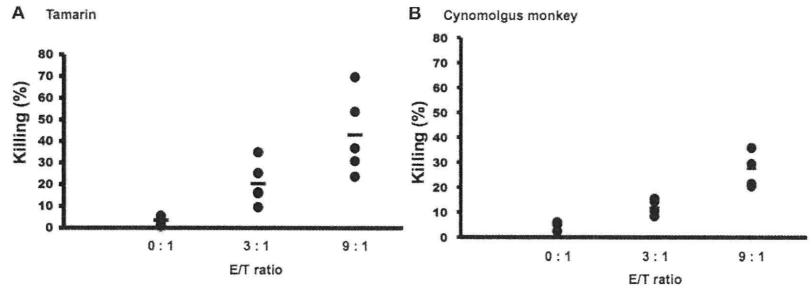

FIGURE 3 | Dose-dependency of killing activity of NK cells in tamarins. (A,B) K562 target cells were stained with CFSE and co-cultured with PBMCs as described in Section "Materials and Methods". CFSE-stained K562 target cells were killed by PBMCs of tamarins and cynomolgus monkeys in a dose-dependent manner. For all experiments, the number of observations used to calculate the mean were $n = 5$. We analyzed statistically whether these killing activities were different between tamarins and cynomolgus monkeys by using StatView software.

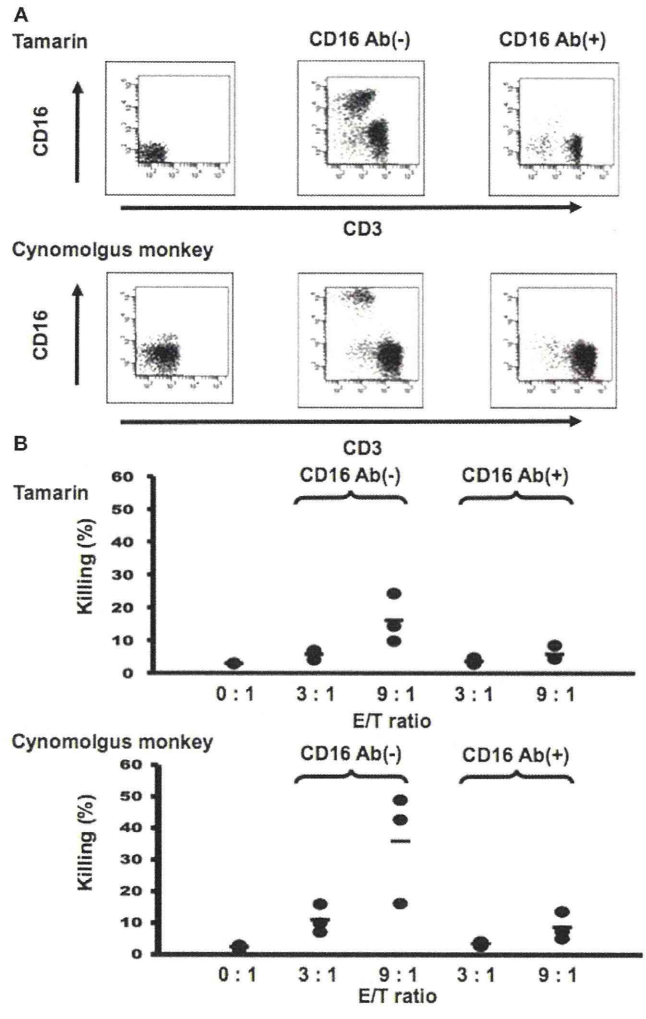

FIGURE 4 | CD16$^+$ cells were a major population with natural killer activity in tamarins. (A) CD16$^+$ cells were depleted from PBMCs by MACS as described in Section "Materials and Methods". CD16$^-$ PBMCs were obtained by negative selection using MACS. **(B)** K562 cells were stained with CFSE and co-cultured with CD16-treated or untreated PBMCs as described in Section "Materials and Methods". Results shown are representative of three independent experiments.